Biochimica et Biophysica Acta 1853 (2015) 453–469

Contents lists available at ScienceDirect

Biochimica et Biophysica Acta

journal homepage: www.elsevier.com/locate/bbamcr

CSN-associated USP48 confers stability to nuclear NF-κB/RelA by trimming K48-linked Ub-chains

Katrin Schweitzer, Michael Naumann *

Otto von Guericke University, Medical Faculty, Institute of Experimental Internal Medicine, 39120 Magdeburg, Germany

ARTICLE INFO

Article history:
Received 17 October 2014
Received in revised form 25 November 2014
Accepted 26 November 2014
Available online 5 December 2014

Keywords:
NF-κB
COP9 signalosome
RelA
Deubiquitinase
CK2
Nuclear protein turnover

ABSTRACT

Diligent balance of nuclear factor kappa B (NF-κB) activity is essential owing to NF-κB's decisive role in cellular processes including inflammation, immunity and cell survival. Ubiquitin/proteasome-system (UPS)-dependent degradation of activated NF-κB/RelA involves the cullin-RING-ubiquitin-ligase (CRL) ECS^{SOCS1}. The COP9 signalosome (CSN) controls ubiquitin (Ub) ligation by CRLs through the removal of the CRL-activating Ub-like modifier NEDD8 from their cullin subunits and through deubiquitinase (DUB) activity of associated DUBs. However, knowledge about DUBs involved in the regulation of NF-κB activity within the nucleus is scarce.

In this study we observed that USP48, a DUB of hitherto ill-defined function identified through a siRNA screen, associates with the CSN and RelA in the nucleus. We show that USP48 trims rather than completely disassembles long K48-linked free and substrate-anchored Ub-chains, a catalytic property only shared with ataxin-3 (Atx3) and otubain-1 (OTU1), and that USP48 Ub-chain-trimming activity is regulated by casein-kinase-2 (CK2)-mediated phosphorylation in response to cytokine-stimulation. Functionally, we demonstrate for the first time the CSN and USP48 to cooperatively stabilize the nuclear pool of RelA, thereby facilitating timely induction and shutoff of NF-κB target genes.

In summary, this study demonstrates that USP48, a nuclear DUB regulated by CK2, controls the UPS-dependent turnover of activated NF-κB/RelA in the nucleus together with the CSN. Thereby USP48 contributes to a timely control of immune responses.

1. Introduction

The ubiquitous transcription factor NF-κB has a decisive function in innate and adaptive immune responses, proliferation and differentiation. Tight control of NF-κB activity is essential to prevent persistent tissue damage by chronic inflammation, representing one major factor contributing to cancer development [1].

The RelA/p50 complex is the prototypic dimeric transcription factor within the NF-κB family. NF-κB is retained in the cytosol by association with inhibitors of NF-κB (IκBs), exemplified by the prototypic family member IκBα, which covers the nuclear localization sequence (NLS) of RelA [2]. In response to various stimuli, initiating the classical pathway of NF-κB activation, IκBα becomes sequentially phosphorylated, ubiquitinated and degraded by the 26S proteasome, resulting in release of NF-κB, its nuclear translocation and ultimately induction of NF-κB target genes. Among the latter is *iκbα* and reaccumulation of IκBα protein represents one major negative feedback loop warranting efficient termination of NF-κB activity through IκBα-dependent nuclear export of RelA [2]. Another important mechanism contributing to timely termination of NF-κB activity is UPS-dependent degradation of RelA in the nucleus/on chromatin [3]. An Ub ligase (Ub-E3) targeting TNF-activated nuclear RelA for degradation is the CRL ECS^{SOCS1}, composed of cullin-2 (Cul2), the adapter proteins Elongin (Elo) B and C, the substrate recognition molecule SOCS1 and the accessory substrate adapter protein "copper metabolism Murr1 domain-containing protein 1" (COMMD1) [4,5].

A superposed regulator of CRLs is the eight subunit (CSN1-8) CSN complex, conserved in the genomes of all eukaryotes [6], which impacts on NF-κB signal transmission at various stages and in response to different triggers [7]. After TNF stimulation, the CSN transiently associates with de novo synthesized IκBα to facilitate its reaccumulation and protect it from sustained UPS-dependent degradation [8]. Upon T cell activation by TCR/CD28 ligation, the CSN associates with the Carma1-Bcl10-Malt1 (CBM) complex, to support efficient activation of the IκB kinase (IKK) complex [9]. Due to a JAB1/MPN/MOV34 (JAMM/MPN^+) motif in CSN5, the CSN, but not isolated CSN5, possesses NEDD8 peptidase (deneddylase) activity [6]. Apart from this, the CSN exerts DUB activity through the association with DUBs, e.g. USP15 [10–12]. Reversible

* Corresponding author at: Otto-von-Guericke-University, Medical Faculty, Institute of Experimental Internal Medicine, Leipziger Str. 44, 39120 Magdeburg, Germany. Tel.: +49 391 67 13227; fax: +49 391 67 13312.
E-mail address: Naumann@med.ovgu.de (M. Naumann).

http://dx.doi.org/10.1016/j.bbamcr.2014.11.028
0167-4889/

neddylation of cullins at a C-terminal Lys residue, conserved in all cullins and Parc, is a critical step in the regulation of CRL assembly and catalytic activity, as well as the proteolytic turnover of CRL subunits [12,13]. While substrate recruitment and cullin neddylation promote CRL activation and substrate ubiquitination, the CSN inhibits CRL activity in vitro. However, since the CSN, through its catalytic activities, protects CRL subunits from autocatalytic degradation [12,14,15] and, independent of its catalytic activities, sequesters fully assembled CRLs, holding them ready in a low activity but immediately accessible state [16], according to the prevailing model [17,18], the CSN is predominantly viewed as positive regulator of the UPS in vivo.

The human genome encodes close to 100 DUBs, which can be subdivided into five families, Ub C-terminal hydrolases (UCHs), Ub-specific peptidases (USPs), ovarian tumor proteases (OTUs), Machado–Joseph disease proteases (MJDs) and JAMM/MPN$^+$ proteases. The first four families belong to the cysteine proteases, whereas JAMM/MPN$^+$ family members are zinc-dependent metalloproteases [19]. While various DUBs from different families participate in the regulation of upstream signaling cascades leading to NF-κB activation [20], knowledge about DUBs involved in the regulation of NF-κB/RelA in the nucleus is scarce. In the present study we show for the first time that the CSN and USP48, a DUB of hitherto largely unknown function, cooperate in the control of ECS^{SOCS1}-dependent RelA ubiquitination to ensure timely induction and shutoff of NF-κB target genes.

2. Results

2.1. RelA and CSN interact in the nucleus

Aiming to explore a potential impact of the CSN on the nuclear turnover of RelA, we initially studied its TNF-induced ubiquitination in subcellular fractions of HeLa cells pulse-stimulated with TNF. Following medium exchange after 15 min, cells were treated with Leptomycin B (LMB) and MG132 to prevent Crm1-dependent nuclear export and proteasomal degradation of RelA. Ubiquitinated RelA (RelA-Ub) accumulated in the nucleus from 1 h after stimulation and predominantly amassed in the insoluble nuclear fraction (N2), enriched for PML and subunits of the 20S proteasome core (Fig. S1A), after 2 h and 4 h (Fig. 1A). Notably, immunoprecipitations (IPs) of RelA from N2 were performed under denaturing conditions, precluding co-IP of associated ubiquitinated proteins. RelA predominantly resided in the cytosol in non-stimulated cells, but translocated into the soluble nuclear fraction (N1) in response to TNF, showing the highest accumulation after 30 min, when IκBα was almost completely degraded in the cytosol. The decline of RelA in N1 from 1 h after stimulation and the concomitant lack of RelA enrichment in N2 are due to accumulation of high molecular weight (HMW) RelA-Ub. Interestingly, nuclear accumulation and an increasing co-IP of the CSN (CSN3) with RelA were concurrently observed in N1 (Figs. 1A and S1B). Notably, inducible association of the CSN with factors of the NF-κB system (IκBα, IKKβ, Bcl10), regulated by CRL- and/or UPS-dependent degradation, has been demonstrated previously [8,9,21,22].

To display the TNF-induced shift of RelA from N1 to N2, cells were transiently transfected with His$_6$-T7-RelA. Overexpressed RelA constitutively localized in N1 and did not further accumulate in response to TNF (Fig. 1B). Moreover, degradation of IκBα was not detectable in the cytosol of RelA-transfected cells due to constitutive NF-κB activity and induction of IκBα de novo synthesis, indicated by strongly increased basal expression of IκBα. In spite of this, TNF induced a movement of His$_6$-T7-RelA from N1 to N2, where it, continuously expressed under the control of the CMV promoter, accumulated. Simultaneously, His$_6$-T7-RelA-Ub amassed almost exclusively in N2 alike, most prominently at late times (Fig. 1B), consistent with data obtained for endogenous RelA (Fig. 1A). There it was detected by antibodies specific for Ub or K48-linked Ub-chains, indicating that ubiquitination labels RelA for degradation via the UPS.

Studying nuclear turnover of endogenous RelA in the presence of LMB but the absence of MG132, repetitive RelA nuclear translocation and RelA-Ub accumulation were observed in N2. Yet, 1 h and 4 h after TNF stimulation RelA-Ub was lost from N2 due to UPS-dependent degradation (Fig. 1C). Renewed accumulation and ubiquitination of RelA in N2 2 h after stimulation is likely due to a second wave of NF-κB activation, even after the single pulse of TNF applied in the experiment. Inherent oscillatory properties of the NF-κB system after its activation by TNF and other stimuli through e.g. induction of both, pro-inflammatory cytokines, as well as negative regulators (IκBs and the DUB A20) have been reported and their biological significance in control of NF-κB-dependent gene induction is subject of debate [23–25]. Like in the previous experiment, RelA-Ub was recognized by antibodies specific for Ub or K48-linked Ub-chains. Interestingly, in the absence of MG132, strongest RelA ubiquitination was observed already at an earlier time (10 min), indicating that subsequent to its nuclear entry RelA becomes rapidly ubiquitinated. Notably, TNF-induced RelA ubiquitination in the nucleus was similarly observed in HEK293 cells (Fig. S1C).

2.2. CSN and ECS^{SOCS1} control RelA ubiquitination and nuclear abundance/turnover

To analyze the impact of the CSN and ECS^{SOCS1} on RelA ubiquitination, we performed transient knockdowns of CSN2 and the ECS^{SOCS1} subunits COMMD1 and EloB. Target-specific knockdown of CSN2 (Fig. S2A) destabilized the CSN complex (Fig. S2B). Concerted modulation of CSN subunit protein expression is in agreement with previous reports [8,26–28]. In response to TNF in the presence of MG132, RelA-Ub accumulation was enhanced in CSN-depleted cells (Fig. 2A), indicating that the CSN antagonizes ubiquitination of RelA. On the contrary, in cells depleted for either COMMD1 or EloB (Fig. 2B, C), RelA ubiquitination was decreased/nearly abolished, consistent with ECS^{SOCS1} being the predominant Ub-E3 for RelA, as suggested previously [4,5]. Studying the impact of the CSN on nuclear abundance and turnover of RelA in TNF-stimulated cells, we observed RelA nuclear accumulation to be delayed and diminished up to 60 min in CSN2-depleted cells, when it peaked in N1. Yet, 2 h and 4 h after stimulation, the clearance of RelA from N1 in the presence of LMB was enhanced (Fig. 2D). In EloB knockdown cells deficient for functional ECS^{SOCS1} in contrast, basal and TNF-induced nuclear accumulation of RelA were enhanced (Fig. 2E). More importantly however, the depletion of RelA from the nucleus, visible from 30 min after TNF stimulation, was diminished, consistent with impaired RelA ubiquitination and UPS-dependent degradation. Instead of efficient clearance from the nucleus, a movement of RelA from N1 to N2 was observed (Fig. 2E).

2.3. CSN directly interacts with RelA and USP48

To identify DUBs counteracting TNF-induced ubiquitination and degradation of nuclear RelA, a siRNA screen was performed, from which USP48 (formerly USP31) [29], a biochemically and functionally largely uncharacterized DUB, emerged as the most promising candidate. Structurally it comprises an N-terminal catalytic domain, three “domains in USPs” (DUSP domains) of unknown function and a C-terminal Ub-like (UBL) domain (Fig. 3G) [30]. Validating this DUB candidate, which had already been linked to NF-κB in one previous study [29], we observed that USP48 predominantly resides in the nucleus (N1) (Fig. S3A, B), where it constitutively co-precipitated with the CSN (Fig. 3A, B). TNF-inducible interactions in contrast occurred between USP48 and RelA (Fig. 3B, C) and between RelA and CSN (Fig. 3A, C), likewise in N1. Control-IPs without IP antibody did not precipitate the analyzed proteins (data not shown). Co-IPs between human purified CSN, recombinant RelA and recombinant full length USP48 (USP48-FL) revealed direct interactions between CSN and USP48 (Fig. 3D) and between CSN and RelA (Fig. 3E) but not between USP48

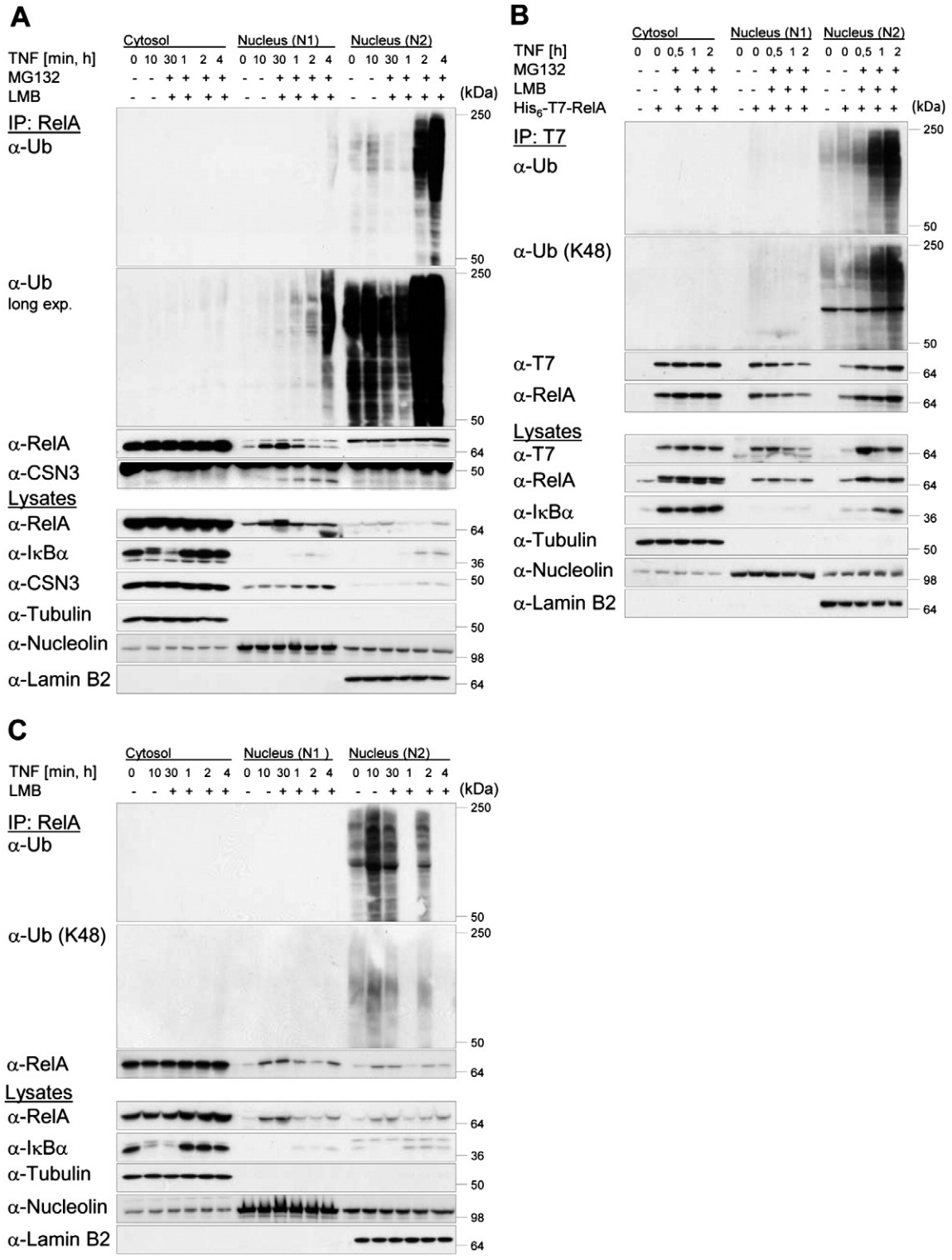

Fig. 1. RelA is ubiquitinated in the nucleus and interacts with the CSN. (A) IP of endogenous RelA from subcellular fractions of HeLa cells 15 min pulse-stimulated with TNF (MG132 and LMB added after 15 min) and harvested at the indicated times in the presence of NEM and OPT. (B) IP of overexpressed epitope-tagged RelA after treatment of cells as described (A). (C) IP of endogenous RelA after treatment of cells as described (A) in the absence of MG132. (A–C) IBs of IPs and subcellular fractions from one representative experiment are shown. Detection of Tubulin (cytosol), Nucleolin (N1) and Lamin B2 (N2) served as control for fraction purity and equal protein load.

and RelA (Fig. 3F), even when the co-IP-direction was reversed (Fig. S3C). Similarly, no direct interaction was detected between RelA and the USP48 catalytic domain (USP48-CD, aa 1–450) (Fig. S3D). It is however possible, that TNF-induced ubiquitination of RelA and/or other yet to be identified inducible PTMs of RelA, USP48 or unknown interaction partners are required to mediate this interaction.

2.4. USP48 stabilizes nuclear RelA through its DUB activity

Next we explored the impact of USP48 on TNF-dependent RelA nuclear translocation, ubiquitination and turnover. TNF-induced degradation and reaccumulation of IκBα were not affected in USP48-depleted cells (Fig. 4A, D, E), indicating unperturbed upstream signaling to NF-κB

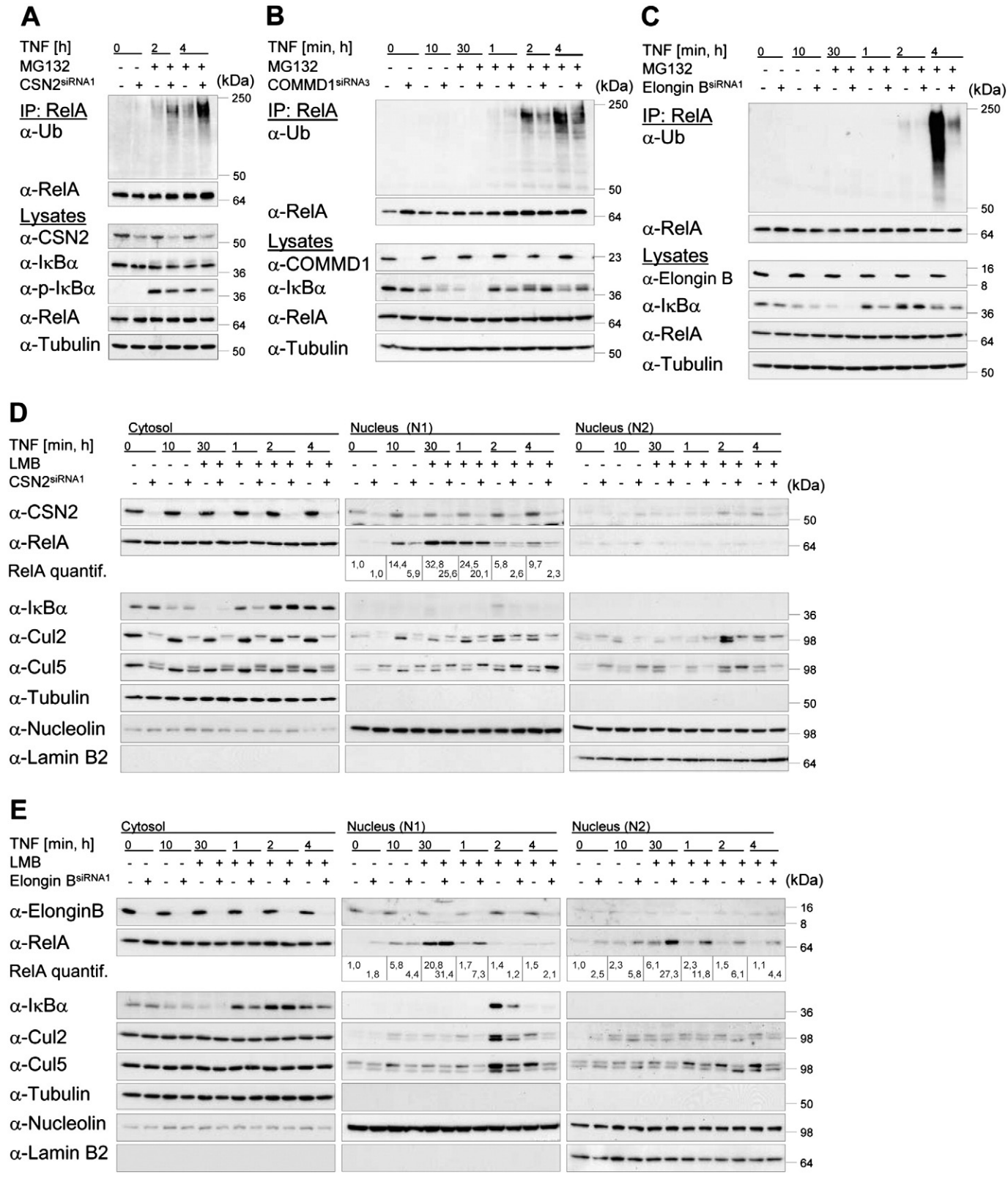

Fig. 2. CSN antagonizes ECS^{SOCS1}-dependent RelA ubiquitination. (A–C) RelA-IP from RIPA lysates after transient knockdown of CSN2 (A), COMMD1 (B) or Elongin B (C). (D, E) Functional inactivation of CSN (D) or ECS^{SOCS1} (E) by transient knockdown of CSN2 or Elongin B affects TNF-induced nuclear translocation and turnover of RelA. (A–E) HeLa cells were 15 min pulse-stimulated with TNF (MG132 and/or LMB added after 15 min) and harvested at the indicated times in the presence of NEM and OPT. IBs of IPs, lysates and subcellular fractions, as indicated, from one representative experiment are shown. Tubulin (cytosol, RIPA lysate), Nucleolin (N1) and Lamin B2 (N2) served as control for fraction purity and/or equal protein load.

activation. Yet, RelA-Ub accumulation in the presence of MG132 was enhanced in HeLa and HEK293 cells (Figs. 4A and S4A). In cells transiently transfected to overexpress USP48-FL, TNF-induced RelA ubiquitination in the nucleus was suppressed. Conversely, cells overexpressing supposedly catalytically dead USP48-FL with the predicted catalytic site Cys converted to Ala ($USP48^{C98A}$) showed enhanced

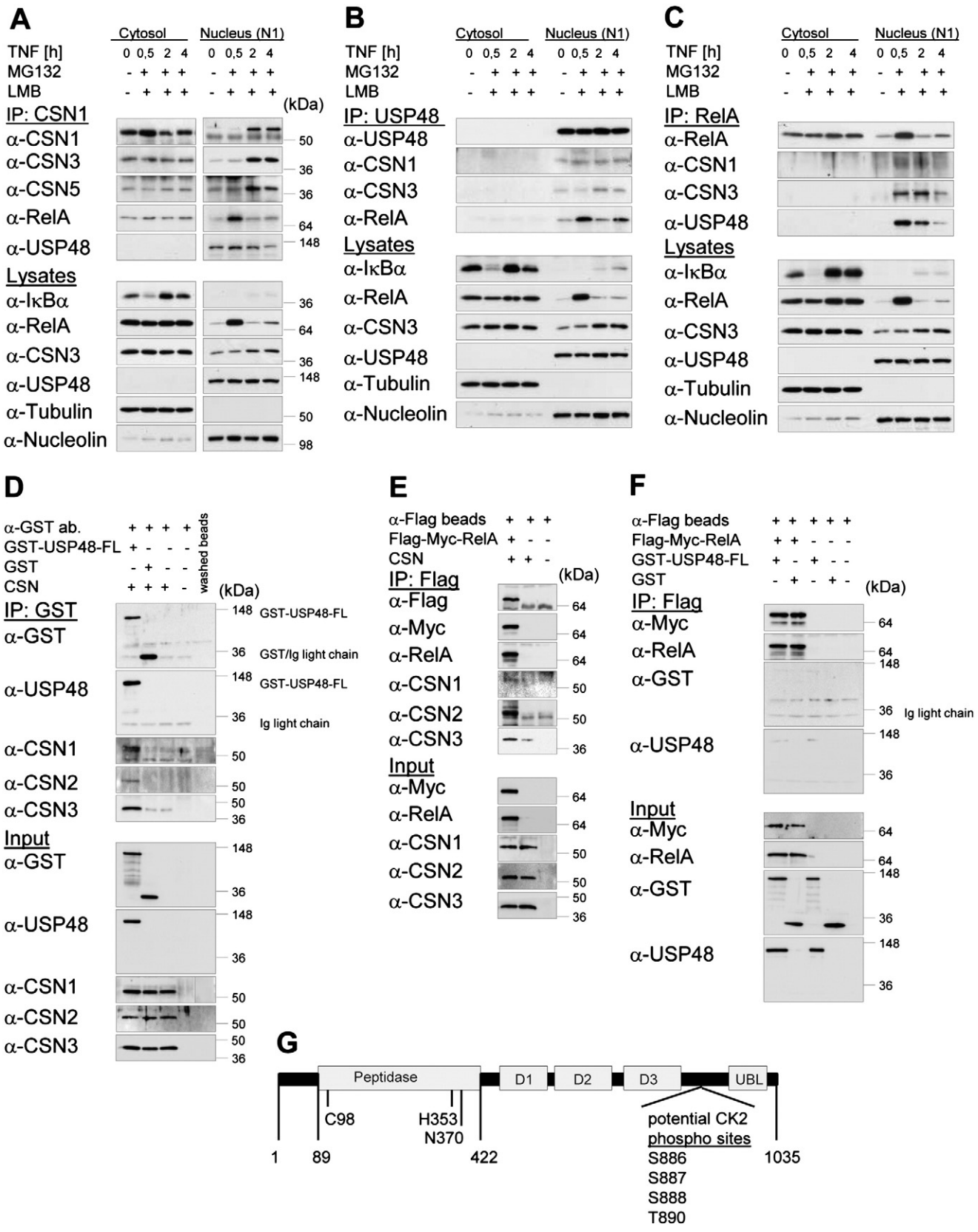

Fig. 3. CSN directly interacts with RelA and USP48. (A–C) IPs, as indicated, from subcellular fractions of HeLa cells 15 min pulse-stimulated with TNF (MG132 and LMB added after 15 min) and harvested at the indicated times in the presence of NEM and OPT. IPs and subcellular fractions were analyzed by IB. The detection of Tubulin (cytosol) and Nucleolin (N1) served as control for subcellular fraction purity and equal protein load. (D–F) Equal molar amounts of recombinant epitope-tagged proteins or human purified CSN, as indicated, were coincubated for 2 h at 4 °C and IPs performed afterwards. Complex formation between coincubated proteins and/or the CSN, as well as protein input were analyzed by IB. (A–F) Results obtained from one representative experiment are shown. (G) Domain structure of USP48. The catalytic triad, consisting of Cys^{98}, His^{353} and Asn^{370}, and predicted high score CK2 phosphorylation sites in the C-term of USP48 are shown. Data stem from Swiss-Prot database and a published report [56]. CK2 phosphorylation site prediction was performed with GPS 2.1 [57].

accumulation of nuclear RelA-Ub (Fig. 4B). Collectively, these data indicated that USP48 inhibits TNF-induced RelA ubiquitination through its DUB activity. An in vitro DUB assay with recombinant USP48-FL and RelA-Ub, immunoprecipitated from nuclear fractions of TNF-stimulated cells, as substrate, confirmed the ability of USP48 to (incompletely) disassemble poly-Ub-chains attached to RelA

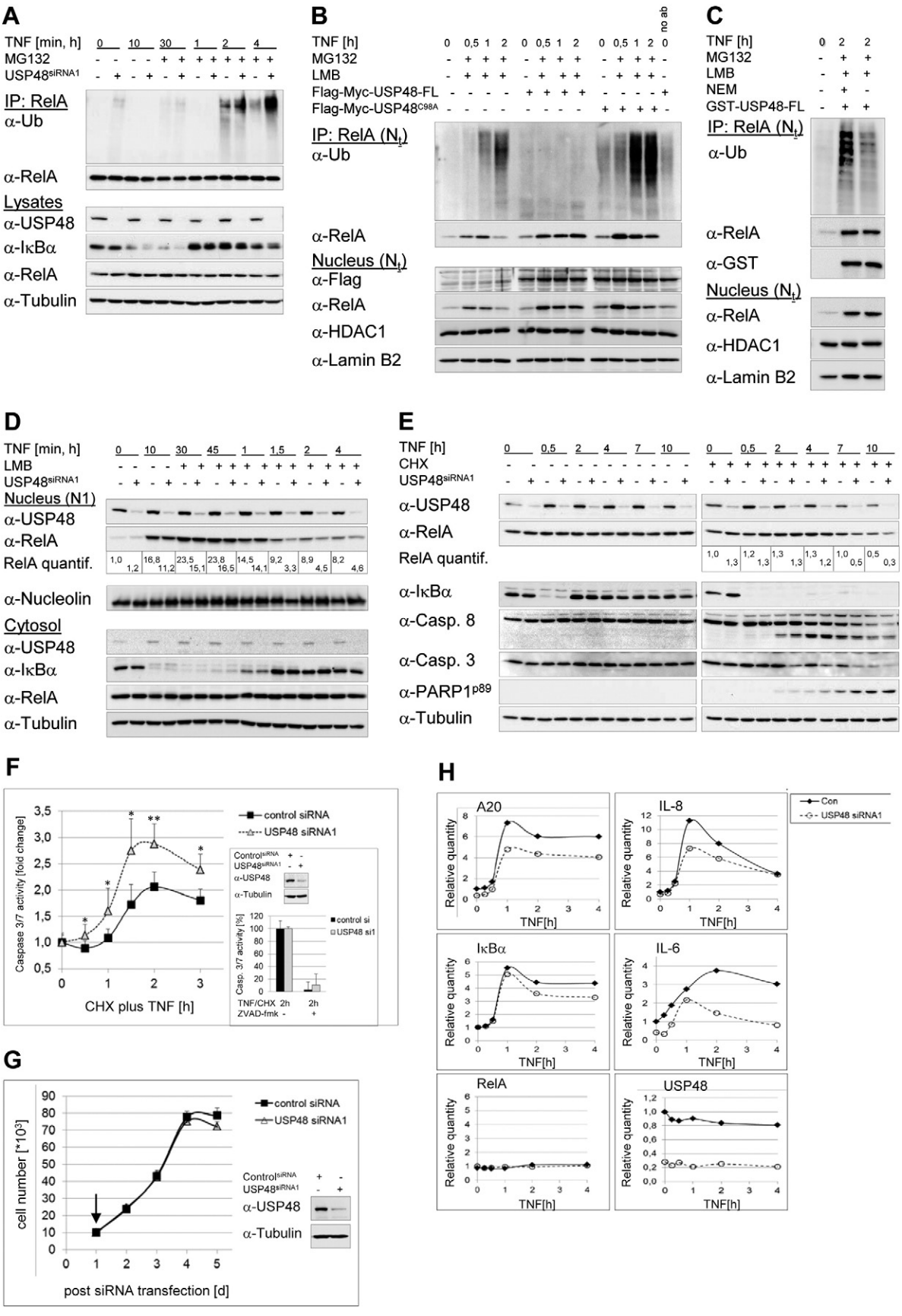

(Fig. 4C). Interestingly, overexpressed USP48 promoted RelA nuclear accumulation 30 min after TNF stimulation independent of catalytic site Cys C98. At later times however, RelA decreased in USP48^{C98A}- and mock-transfected cells due to ubiquitination and movement into the HMW fraction, whereas its amount remained constant in USP48-FL-transfected cells (Fig. 4B). In USP48-depleted cells, TNF-induced RelA nuclear accumulation was reduced at early times. From 1.5 h after stimulation, the clearance of RelA from N1 in the presence of LMB was accelerated, both likely due to enhanced RelA ubiquitination and proteasomal degradation (Fig. 4D). Of note, USP48 similarly affected RelA nuclear accumulation and turnover in response to TNF and IL-1β (Fig. S4B, D). Enhanced RelA nuclear turnover in USP48-depleted cells was inhibited by treatment of cells with MG132 (Fig. S4C, E). USP48-dependent protection of RelA from degradation was confirmed in experiments with the protein synthesis inhibitor cycloheximide (CHX). While total amounts of RelA did not change in response to TNF, a decrease of RelA was observed after co-treatment of cells with CHX from 7 h after TNF stimulation, which was more prominent in USP48-depleted cells (Fig. 4E). Apart from this, accelerated induction of apoptosis manifested in USP48-depleted cells co-treated with TNF and CHX, as evidenced by accelerated cleavage (activation) of pro-caspases 8 and 3 and caspase substrate PARP1 (Fig. 4E). Protection of cells against TNF/CHX-induced apoptosis by USP48 was confirmed in a biochemical assay for activation of executioner caspases 3 and 7 (Fig. 4F). Caspase activation was efficiently inhibited by cell pre-treatment with pan-caspase inhibitor ZVAD-fmk (Fig. 4F). Depletion of USP48 by itself did not affect cell proliferation and viability (Fig. 4G). Consistent with diminished TNF-induced nuclear accumulation and accelerated degradation of RelA in USP48-depleted cells, induction of NF-κB target gene expression was decreased and/or delayed, whereas gene expression of *rela* was unaffected (Fig. 4H). Notably, diminished induction of *tnfaip3* (A20) in USP48-depleted cells could be confirmed at the protein level (Fig. S4B). NF-κB-dependent induction of A20, a DUB protecting cells from apoptosis through inhibition of caspase activation [31,32], thus provides a potential link between promotion of RelA stability and cell protection from apoptosis by USP48.

2.5. USP48 preferentially trims long Ub-chains

We then characterized USP48 DUB activity in more detail. While no catalytic activity of recombinant USP48 could be detected in the DUB-Glo® Protease Assay, it was detectable for USP48-FL and USP48-CD, when the Ub C-terminal peptide-based substrate provided with the kit was replaced by Ub-aminoluciferin (Ub-AML) (Figs. 5A and S5-1E, F). However, USP48 DUB activity was lower by a factor of about 10 compared to other USPs and 100 compared to UCHL3, a DUB with high peptidase activity (Figs. 5A and S5-1A–F). While UCHs professionally process Ub precursors and remove small adducts from the C-terminal Gly of Ub, most other DUBs preferentially cleave isopeptide over peptide bonds [30]. USP48^{C98A}, with the proposed catalytic site Cys mutated to Ala, showed weak catalytic activity in this assay as well (Figs. 5A and S5-1G).

Ub-chains in FRET-based Ub_2-substrates are linked via true isopetide bonds between the C-terminal carboxylate of the distal Ub and the ε-amino group of one of the three internal Lys residues (K48, K63 or K11) of the proximal Ub, reflecting the as yet best studied Ub-chain linkage types in cells. Nevertheless, recombinant USP48-FL and USP48-CD hydrolyzed these substrates with very low efficiency compared to other USPs as well. Yet, all linkage types were hydrolyzed to some extent, with a preference for K11-linked Ub-chains (Figs. 5B and S5-2A–G). While USP48-FL cleaved K48- and K63-linked Ub_2-substrates equally well, the latter were hardly cleaved by USP48-CD. UCHL3, used as negative control, did not hydrolyze Ub_2-substrates at all (Fig. S5-2F), consistent with a previous report [33]. Interestingly, all USPs tested, except USP48, most efficiently hydrolyzed K63-linked Ub_2-substrates. But, while USP15 hardly cleaved K48-linked Ub_2, this was favored over K11-linked Ub_2 by USP5 and USP7. Together with published data [30] these data indicate that although most USPs examined are promiscuous, hydrolyzing Ub-chains of all linkage types, preferences for distinct topologies exist.

Low DUB activity of USP48 towards Ub-AML and FRET-based Ub_2-substrates but its ability to counteract UPS-targeting of RelA, led us to reason if USP48 might preferentially trim long Ub-chains ($\geq U_4$), a property previously observed for Atx3 [34]. K48-linked Ub_4 attached to substrates represents the minimal target signal for proteasomal degradation [35]. Thus, we examined the ability of recombinant USP48 to hydrolyze Ub_4 and Ub_{3-7}-chains of different topology. Very weak disassembly only of K63- and K11-linked Ub_4 was detected for USP48-CD, whereas USP48-FL hydrolyzed Ub_4 of all examined linkage types more efficiently (Fig. 5C). Both, USP48-FL and USP15 cleaved M1-linked Ub_4 worst. Apart from the latter, USP48-FL hydrolyzed Ub_4 of all studied topologies almost equally well, whereas USP15 hardly hydrolyzed K48-linked Ub_4 alike, consistent with data obtained with FRET-based Ub_2-substrates (Fig. 5B). UCHL3 did not digest Ub_4 at all, as reported previously [36].

Directly comparing the ability of USP48-FL to hydrolyze K48-linked Ub_4 and Ub_{3-7}-chains, we observed it to much more efficiently trim but not completely disassemble UB_{3-7}-chains (Fig. 5D). Accumulation of Ub_1 became most evident in SYPRO-Rubi-stained gels. Ub-chain disassembly was inhibited by NEM, indicating its dependence on DUB activity (Fig. 5D). In contrast to USP48-FL, USP48-CD neither hydrolyzed K48-linked Ub_4 nor Ub_{3-7}-chains noticeably (Fig. 5E). Finally, we directly compared USP48-FL with USP48-CD and USP48^{C98A} in its efficiency to trim K48-linked Ub_{3-7}-chains (Fig. 5F, G). While Ub-chain trimming, evidenced by accumulation of Ub_2 and Ub_1 and a decreasing amount of long Ub-chains ($>Ub_4$), was consistently observed for USP48-FL and inhibited by NEM, neither USP48^{C98A} (Fig. 5F) nor USP48-CD (Fig. 5G) hydrolyzed these Ub-chains at all. Similar results were obtained with overexpressed USP48 variants after their IP from total cell lysates (Fig. S5-3A). K48-linked Ub_4 was not hydrolyzed at all by overexpressed USP48-CD and USP48^{C98A} alike (Fig. S5-3B). These results strongly suggest Ub-chain-trimming by USP48 to essentially depend on sequence motifs outside the CD and, in contrast to its peptidase activity (Fig. 5A), on the proposed catalytic site Cys C98.

Fig. 4. USP48 stabilizes RelA by deubiquitination. (A, B) RelA-IP from RIPA lysates (A) or total nuclear fractions (B) of HeLa cells 15 min pulse-stimulated with TNF (MG132 and/or LMB added after 15 min) and harvested at the indicated times in the presence of NEM and OPT. (A, D–H) Transient knockdown of USP48. (B) Overexpression of epitope-tagged USP48-FL or USP48^{C98A}, with the proposed catalytic site Cys mutated to Ala. (C) In vitro DUB assay. RelA-IPs from total nuclear fractions of HeLa cells 2 h stimulated with TNF as described (A, B) were incubated for 2 h with recombinant GST-USP48-FL in the presence or absence of NEM. (D) Subcellular fractionation of HeLa cells stimulated with TNF as described (A, B) after transient knockdown of USP48. (E) HeLa cells were treated or not with CHX directly prior to TNF stimulation for indicated times. Apoptosis induction was determined by IB-detection of pro-caspase cleavage (activation) and detection of the 89 kDa fragment of caspase-cleaved PARP-1. (D, E) Changes in signal intensity of RelA in the nucleus (C) or RIPA lysates of cells treated with TNF and CHX (D) were quantified and numbers for relative changes indicated. RelA signal intensity in non-stimulated control cells was arbitrarily set 1. (A–G) IBs of samples, as indicated, from one representative experiment are shown. Tubulin (Cytosol), Nucleolin (N1), HDAC1 (total nucleus, N_t) and Lamin B2 (N2, N_t) were used as marker proteins and detected for control of equal protein load. (F) After 1 h pre-treatment or not with pan-caspase inhibitor ZVAD-fmk, HeLa cells were subjected to TNF/CHX treatment for the indicated times and subsequently to Caspase 3/7-Glo® Assay. Fold changes in caspase activity (mean ± s.d.) compared to untreated cells are shown (*, $p \leq 0.05$; **, $p \leq 0.01$; $n = 3$). (G) Proliferation assay. Equal cell numbers were seeded in quadruplicate 1 day after siRNA treatment. Every 24 h cell numbers (mean ± s.d.) were determined with Cell Titer-Glo® Luminescent Cell Viability Assay. (F, G) Knockdown efficiency was proved by IB analysis of RIPA cell lysates. (H) RT-qPCR analysis of NF-κB target gene induction in HeLa cells stimulated with TNF for the indicated times after transient knockdown of USP48. Relative changes in gene expression compared to non-stimulated control cells in representative experiments ($n = 3$) are shown. Data points represent the mean of 2 replicates run in parallel.

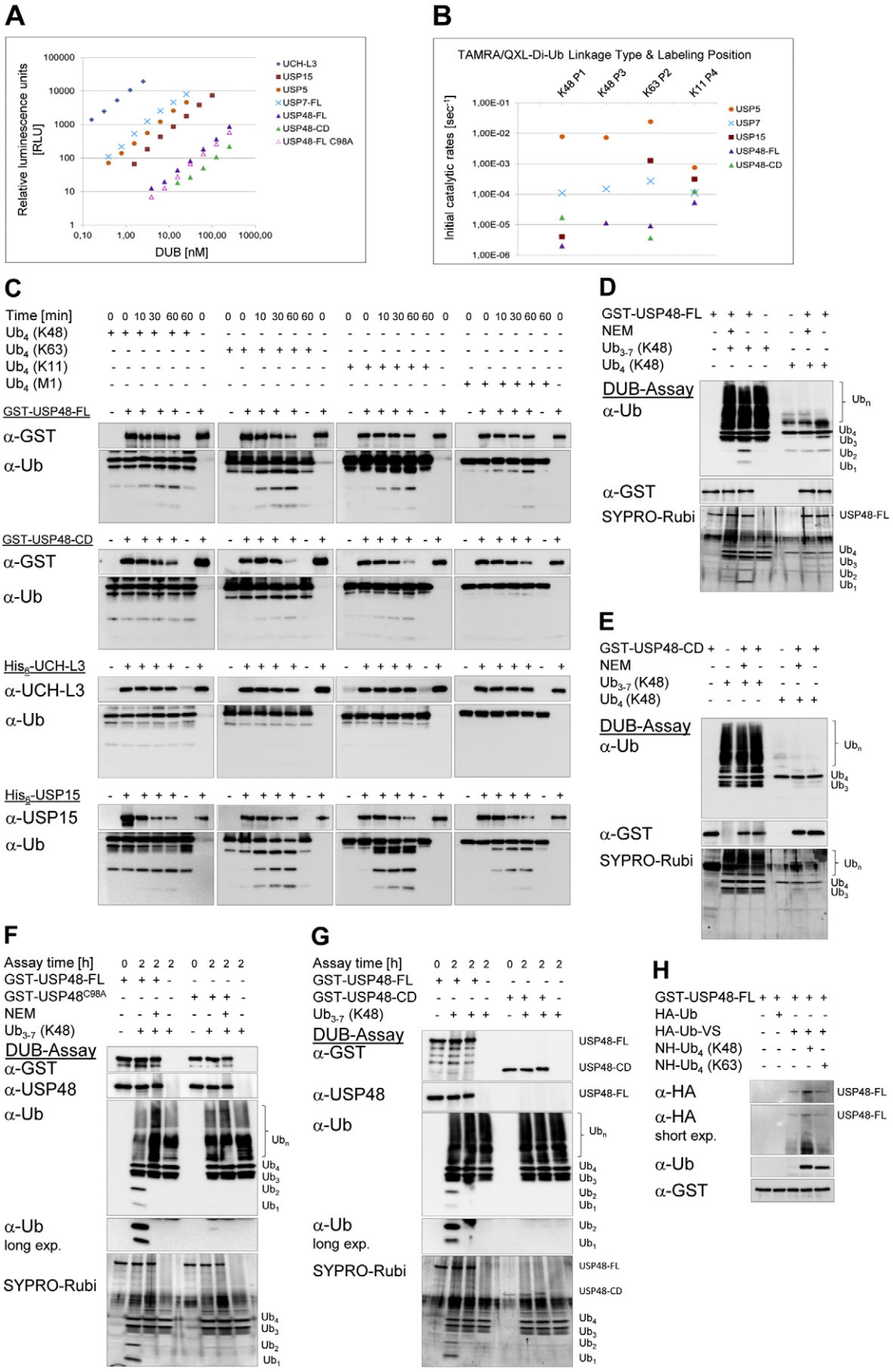
A
Relative luminescence units [RLU]
DUB [nM]
UCH-L3
USP15
USP5
USP7-FL
USP48-FL
USP48-CD
USP48-FL C98A
B
TAMRA/QXL-Di-Ub Linkage Type & Labeling Position
K48 P1
K48 P3
K63 P2
K11 P4
Initial catalytic rates [sec-1]
USP5
USP7
USP15
USP48-FL
USP48-CD
C
Time [min]
Ub4 (K48)
Ub4 (K63)
Ub4 (K11)
Ub4 (M1)
GST-USP48-FL
α-GST
α-Ub
GST-USP48-CD
His6-UCH-L3
α-UCH-L3
His6-USP15
α-USP15
D
GST-USP48-FL
NEM
Ub3-7 (K48)
Ub4 (K48)
DUB-Assay
α-Ub
α-GST
SYPRO-Rubi
USP48-FL
E
GST-USP48-CD
F
Assay time [h]
GST-USP48-FL
GST-USP48C98A
α-USP48
α-Ub long exp.
G
GST-USP48-CD
H
HA-Ub
HA-Ub-VS
NH-Ub4 (K48)
NH-Ub4 (K63)
α-HA
α-HA short exp.

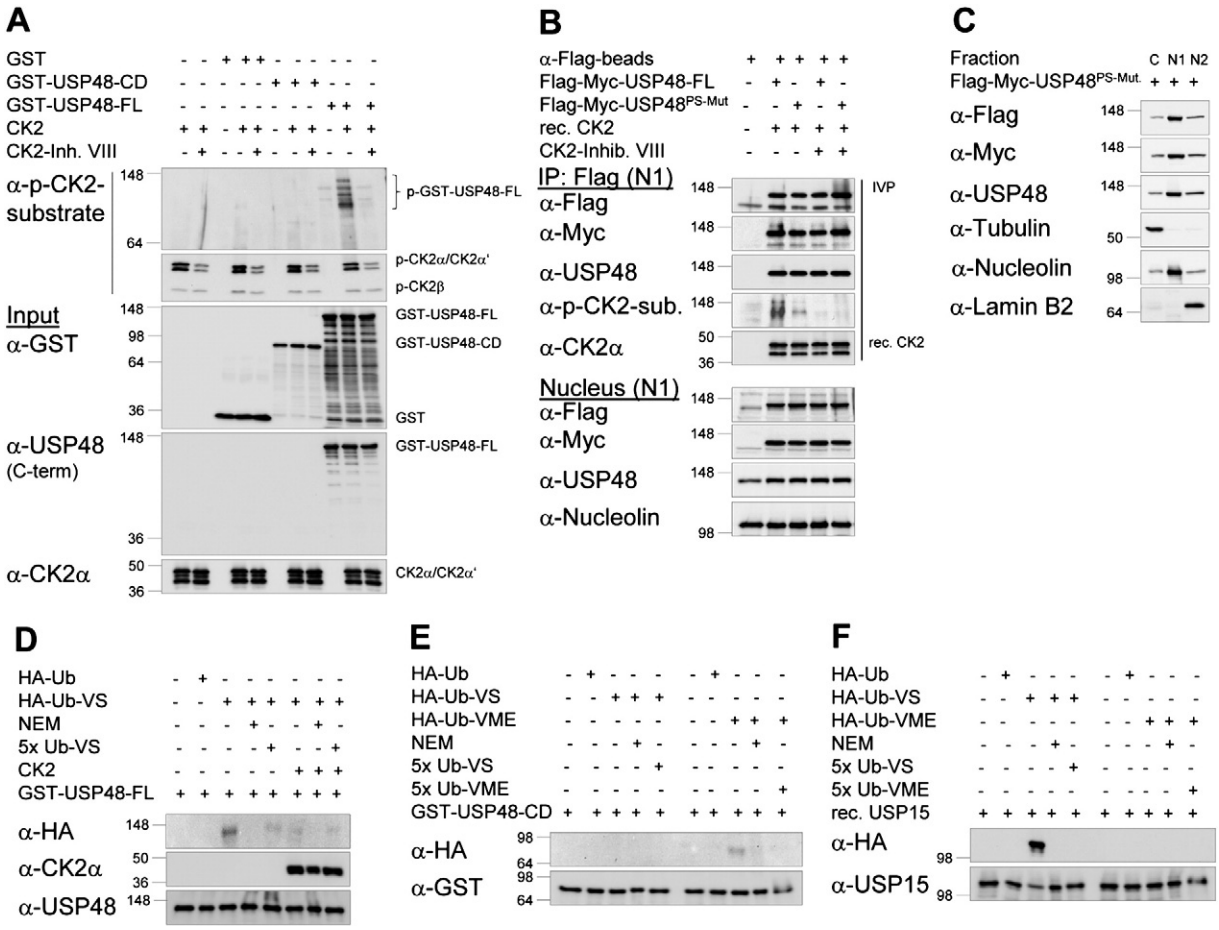

Fig. 6. USP48 catalytic activity is regulated by CK2 (A, B). In vitro CK2 kinase assay with either recombinant GST-USP48-FL or GST-USP48-CD (A) or either epitope-tagged USP48-FL or a USP48-FL four phosphosite mutant (USP48$^{PS\text{-}Mut.}$, as specified in Fig. 3G), immunoprecipitated from N1 fractions of HeLa cells after overexpression (B), in the presence or absence of CK2 inhibitor VIII. (C) Subcellular location of overexpressed epitope-tagged USP48$^{PS\text{-}Mut.}$. (D–F) Trap-tag-labeling of recombinant GST-USP48-FL (D), GST-USP48-CD (E) or USP15 (F) with HA-tagged Ub-derived suicide probes, as indicated, in the presence or absence of either NEM or an excess of untagged suicide probe. Reactions with HA-Ub, lacking a thiol-reactive group, were included as control. (D) GST-USP48-FL was additionally subjected to a CK2 kinase reaction prior to and during trap-tag-labeling. (A–F) IBs of samples, as indicated, from one representative experiment are shown. Tubulin (cytosol), Nucleolin (N1) and Lamin B2 (N2) served as marker proteins for subcellular fractions (B, C) and were detected for control of fraction purity (C) and/or equal protein load.

The predilection of USP48-FL to hydrolyze long K48-linked Ub-chains implicated that it might be activated by Ub-chain-binding through sequence motifs outside the CD. Thus, we subjected it to trap-tag-labeling reactions with a HA-Ub-derived suicide probe in the presence or absence of K48- or K63-linked non-hydrolysable (NH) Ub_4. In these probes, Ub, serving as affinity trap for DUBs, is coupled via its C-term to a thiol-reactive group (vinylsulfone (VS) or vinylmethylester (VME)), which attacks and covalently modifies the DUB catalytic site Cys, thus adding a HA-tag to trapped (catalytically active) DUBs. Labeling of USP48-FL with HA-Ub-VS was enhanced in the presence of K48- but not K63-linked NH-Ub_4 (Fig. 5H), suggesting its selective activation through association with K48-linked Ub_4. Enhanced labeling of USP48-FL was accompanied by decreased DUB stability, as indicated by the accumulation of low MW smear (Fig. 5H).

2.6. USP48 catalytic activity is regulated by CK2

In the C-term USP48 possesses high score CK2 phosphorylation sites (Fig. 3G). Thus we reasoned if CK2-mediated phosphorylation might affect USP48 catalytic activity. The ability of CK2 to phosphorylate USP48 at C-terminal sites was confirmed in kinase assays with recombinant USP48 variants, tagged at the N-term with GST (Fig. 6A). While USP48-FL was phosphorylated by CK2, this was not the case for GST or USP48-CD. Phosphorylation of USP48-FL and CK2α subunits themselves was inhibited by CK2 inhibitor VIII (Fig. 6A). Again, we consistently observed USP48-FL instability indicated by highly abundant low MW smear. The latter was more prominently detected with a GST-specific antibody than an antibody against the USP48 C-term, suggesting USP48 truncation to proceed from the C-term (Fig. 6A).

Fig. 5. USP48 preferentially hydrolyzes long K48-linked Ub-chains. (A) Hydrolysis of Ub-AML (250 nM) by various recombinant USPs and UCHL3 in dependence of DUB concentration. Results from representative experiments (n = 2–3), each with two replicates run in parallel are shown. Also refer to figure S5-1A–G. (B) Initial catalytic rates of recombinant USPs for the hydrolysis of TAMRA/QXL570 Ub_2-substrates of different Ub-linkage types (100 nM) are compared. P1–P4 refers to the position of fluorophore (TAMRA) and quencher (QXL570) in the Ub_2-substrates. Data points represent the mean of 2–3 independent measurements, each with two replicates. Also refer to figure S5-2A–G. (C–G) In vitro DUB assays with recombinant DUBs, as indicated. (C) Kinetics of the hydrolysis of Ub_4 of various linkage types by the indicated DUBs. (D, E) Comparative Ub_4/Ub_{3-7} hydrolysis by either GST-USP48-FL (D) or GST-USP48-CD (E) in the presence or absence of NEM within 1.5 h. (F, G) Comparative analysis of K48-linked Ub_{3-7} hydrolysis by recombinant GST-USP48-FL and either the catalytic site Cys mutant GST-USP48^{C98A} (G) or GST-USP48-CD (H) in the presence or absence of NEM. (H) HA-Ub-VS-Labeling of GST-USP48-FL in the presence or absence of NEM and K48- or K63-linked non-hydrolysable (NH) Ub_4. (C–H) IBs or SYPRO-Rubi gel stains of samples, as specified, from one representative experiment are shown.

Phosphorylation of USP48 at its C-terminal CK2 consensus sites was evidenced in in vitro phosphorylation assays with recombinant CK2 and epitope-tagged USP48 variants, which, after overexpression, had been immunoprecipitated from N1 fractions of HeLa cells. While CK2 efficiently phosphorylated USP48-FL, only marginal phosphorylation of the USP48-FL CK2 phosphosite mutant (USP48$^{PS\text{-}Mut.}$) with all

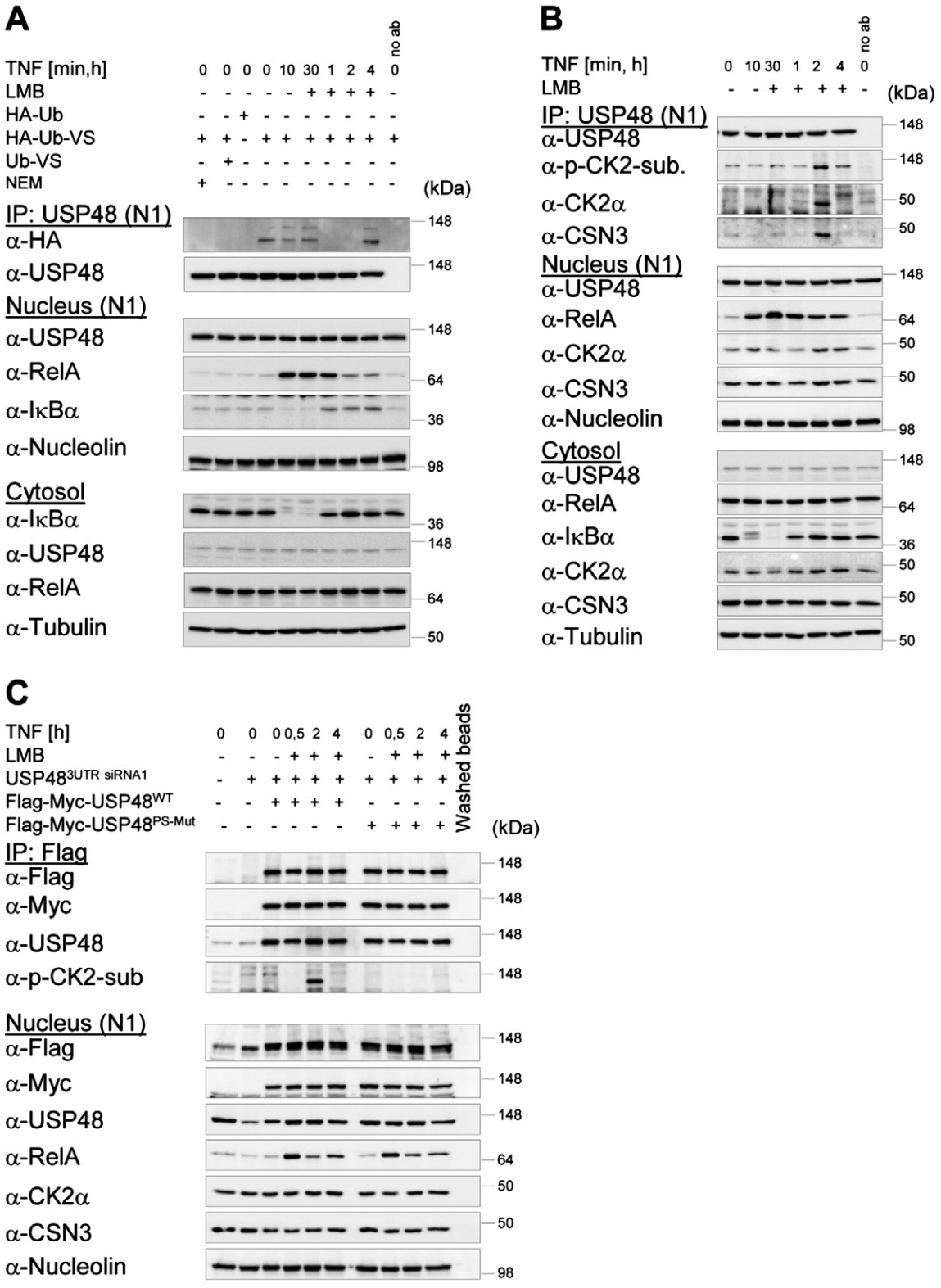

Fig. 7. USP48 becomes phosphorylated at its C-terminal CK2 consensus sites in response to TNF. (A) HA-Ub-VS-labeling of endogenous USP48 is modulated by TNF. (B) USP48 is phosphorylated by CK2 in response to TNF and interacts with CK2 and CSN. (C) USP48 becomes phosphorylated at its C-terminal CK2 consensus sites in response to TNF. (A–C) IP of endogenous USP48 (A, B) or overexpressed epitope-tagged USP48 variants, as indicated, after knockdown of endogenous USP48 (C) from N1 fractions of HeLa cells 15 min pulse-stimulated with TNF (LMB added after 15 min) and harvested at the indicated times. (A–C) IBs of samples, as indicated, from one representative experiment are shown. Tubulin (cytosol) and Nucleolin (N1) served as marker proteins for subcellular fractions, as indicated, and were detected for control of equal protein load.

consensus sites mutated to Ala was observed (Fig. 6B). Of note, combined mutation of these sites did not perturb correct subcellular localization of USP48$^{PS\text{-}Mut.}$ (Fig. 6C).

To study the impact of CK2-mediated phosphorylation on USP48 catalytic activity, we performed trap-tag-labeling of recombinant USP48 in the presence or absence of CK2. Labeling of USP48-FL was only achieved with HA-Ub-VS. HA-Ub was ineffective, as expected, and HA-Ub-VS-labeling could be suppressed by preincubation of USP48 with NEM or a 5-fold excess of non-tagged Ub-VS (Fig. 6D). When USP48-FL was subjected to an in vitro kinase assay prior to and during the labeling reaction, labeling was suppressed indicating that phosphorylation of USP48 in the C-term changes its catalytic activity (see below). Residual labeling of USP48-FL preincubated with CK2 could be suppressed by NEM but not a 5-fold excess of Ub-VS (Fig. 6D). USP48-CD could only be labeled with HA-Ub-VME (Fig. 6E) and this was inhibited by preincubation with either NEM or a 5-fold excess of Ub-VME. The different amenability of USP48-FL and USP48-CD for different thiol-reactive suicide probes indicates regions outside the CD of USP48 to affect the 3-D structure of the latter in the full length protein. Overall, labeling efficiency of USP48 variants was low compared to USP15, which could be efficiently labeled with HA-Ub-VS but not HA-Ub-VME (Fig. 6F), likely reflecting USP48's low capability to cleave Ub_1-substrates (Ub-AML), as well as short Ub-chains (Fig. 5A–C).

HA-Ub-VS-labeling was finally applied again to trace the catalytic activity of endogenous USP48 immunoprecipitated from N1 fractions of HeLa cells. Weak but constitutive labeling of USP48 was lost 1 h and 2 h after TNF stimulation but reappeared after 4 h (Fig. 7A), indicating modulation of USP48 catalytic activity in response to TNF. The labeled band of lower MW likely represents C-terminally truncated USP48 generated during the labeling reaction (Fig. 7A). In support of a functional role of CK2 in the regulation of USP48 catalytic activity, phosphorylation of USP48 at CK2 consensus sites as well as co-IP of CK2α and CSN (CSN3) were observed 2 h after TNF stimulation (Fig. 7B) concurrent with the loss of USP48 HA-Ub-VS-labeling (Fig. 7A). USP48 phosphorylation at its C-terminal CK2 phosphorylation sites in response to TNF was confirmed after knockdown of endogenous USP48, followed by reexpression of either siRNA-resistant USP48-FL^{WT} or USP48$^{PS\text{-}Mut.}$, the latter of which did not become modified (Fig. 7C).

2.7. CK2-mediated phosphorylation of USP48 enhances its Ub-chain trimming activity

Knowing about the preference of USP48 to trim long K48-linked Ub-chains, relevant for UPS-dependent turnover of nuclear RelA, we also analyzed the impact of CK2 and TNF on its ability to disassemble K48-linked Ub_{3-7}-chains. In contrast to HA-Ub-VS-labeling of USP48, which was (transiently) lost after TNF stimulation and upon CK2-mediated phosphorylation (Fig. 7A), phosphorylation of USP48 in response to 2 h TNF stimulation or with recombinant CK2 in vitro enhanced its Ub-chain trimming activity (Fig. 8A–C) and this was inhibited by NEM (Fig. 8A, C) and CK2 inhibitor VIII (Fig. 8B). These results indicate that CK2-mediated phosphorylation of USP48 at its C-terminal CK2 consensus sites and its binding to K48-linked Ub-chains (Fig. 5H), both of which promote USP48 Ub-chain-trimming activity, trigger a conformational rearrangement in USP48/USP48's CD, thereby facilitating the trimming of long K48-linked Ub-chains but simultaneously disabling peptidase activity towards Ub_1-substrates and hydrolysis of short Ub-chains ($\leq Ub_4$).

3. Discussion

In the present study we provide first direct evidence for USP48 DUB activity and a profound characterization of catalytic properties and physiologic function of this as yet ill-characterized DUB predominantly localized in the nucleus. We demonstrate that (I) USP48 preferentially trims long (K48-linked) Ub-chains, an as yet unique property within the USP family, (II) CK2 phosphorylates USP48 at C-terminal CK2 consensus sites, thereby enhancing its Ub-chain-trimming activity (III) USP48 and CSN directly interact in the nucleus, where they cooperate in the control of nuclear accumulation and ECS^{SOCS1}-dependent RelA ubiquitination, thus contributing to timely proteasomal degradation of RelA.

3.1. USP48 has unique catalytic properties within the USP family

We demonstrate for the first time that purified recombinant USP48, a DUB of hitherto largely unknown physiologic function, is catalytically active and has unique catalytic properties within the USP family. Most remarkable among these is the high efficiency of USP48-FL but not USP48-CD or the catalytic site Cys mutant USP48^{C98A} to trim but not completely disassemble long K48-linked unanchored Ub-chains (Figs. 5D–G and S5-3A, B). This property contrasts with the low peptidase activity towards Ub-AML (Figs. 5A and S5-1A–G) and the low isopeptidase activity towards FRET-based Ub_2-substrates (Figs. 5B and S5-2A–G) and unanchored Ub_4 (Fig. 5C). The ability to efficiently trim long ($>Ub_4$), yet to largely spare short (K48-linked) Ub-chains ($\leq Ub_4$) clearly distinguishes USP48 from USP7, recently described as another DUB antagonizing ubiquitination of nuclear/promoter-bound RelA [37]. In contrast to USP48, USP7 efficiently cleaves Ub-AML and FRET-based Ub_2-substrates, the latter however to some extend depending on the Ub linkage type. Furthermore, USP7 poorly disassembles long K48-linked Ub-chains ($\geq Ub_4$) attached to model substrates in vitro but instead efficiently removes short Ub-chains ($<Ub_4$) and mono-Ub from substrates [38].

3.2. Catalytic properties of USP48 partially resemble those of Atx3 and Otu1

Catalytic properties similar to USP48 have, as yet, only been reported for the MJD family DUB Atx3 [34] and the OTU family DUB Otu1 [39,40]. Atx3 consists of an N-terminal catalytic Josephin domain and two Ub interaction motifs (UIMs) in the C-terminal half of the protein, followed by a polyglutamine domain and, depending on the splice variant, a third UIM [41]. In Atx3, like USP48 poised to trim long K48-linked Ub-chains but to spare short Ub-chains [34], the UIMs are reportedly required to efficiently bind poly-Ub-chains and to protect short Ub-chains ($\leq Ub_{4-6}$) from disassembly, as well as a ubiquitinated model substrate from capture and degradation by the proteasome. Notably, model substrate stabilization by Atx3 was shown to be independent from its catalytic activity, which however trimmed substrate-attached poly-Ub-chains down to Ub_{4-6} [34]. Similarly, overexpressed USP48^{C98A}, lacking Ub-chain-trimming activity (Figs. 5F and S5-3A), supported TNF-induced RelA nuclear accumulation as effectively as USP48-FL (Fig. 4B, 30 min TNF), likely through the occupation of short Ub-chains (up to Ub_4) attached to RelA, thereby protecting it from capture by the proteasome. In contrast to USP48-FL however, due to its inability to trim long Ub-chains, it did not prevent a decrease of nuclear RelA from 1 h after TNF stimulation due to polyubiquitination and movement into the HMW fraction. Yet, unlike Atx3, USP48 does not possess any known Ub-binding domain except the USP domain. But it is tempting to speculate that the three DUSP domains in the C-terminal half of USP48 are unrecognized Ub-binding domains. USP48 is the only USP possessing three DUSP domains, some other USPs possessing two (USP20 and USP33) or at least one of them (USP11, USP15 and USP32) [30].

While Otu1 preferences for Ub-chain length and linkage type resemble those of USP48 and Atx3 [39,40], Otu1 only consists of an N-terminal Ub regulatory X (UBX)-type UBL, recruiting it to the AAA ATPase Cdc48/p97/VCP [39,40], the catalytic OTU domain and a C-terminal zinc finger [30]. Of interest in relation to USP48, bidentate substrate-binding based on two different Cys residues, (I) the catalytic site Cys, susceptible for modification/inactivation by Ub-aldehyde but

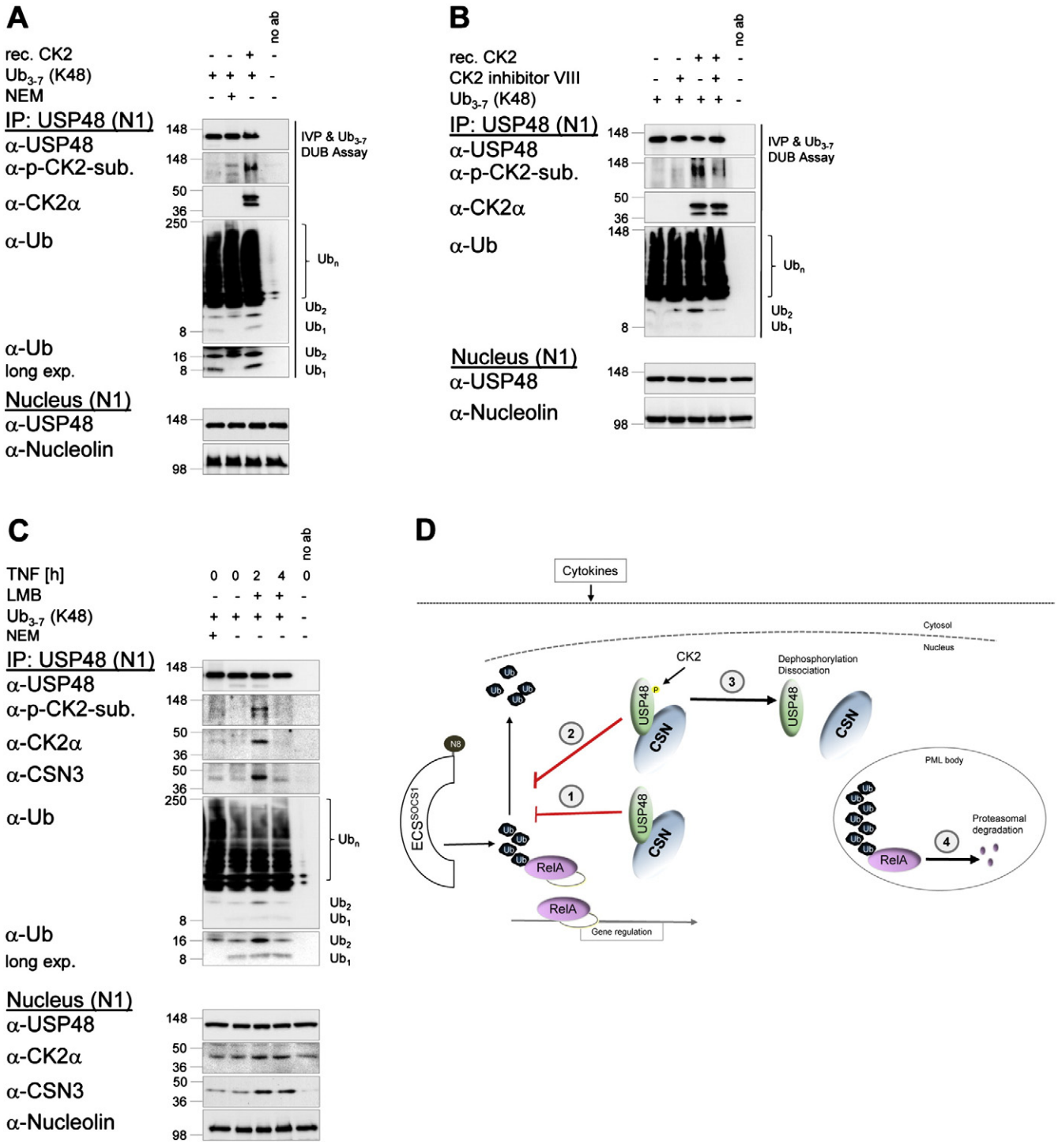

Fig. 8. CK2-mediated phosphorylation promotes USP48 Ub-chain trimming activity. (A–C) DUB assays with USP48 immunoprecipitated from N1 fractions of non-stimulated HeLa cells (A,B) or HeLa cells stimulated with TNF for the indicated times (C) and K48-linked Ub_{3-7} chains as substrate in the presence or absence of either NEM (A, C) or CK2 inhibitor VIII. IBs of samples, as indicated, from one representative experiment are shown. Nucleolin (N1) was used as marker protein and detected as control for equal protein load. (A, B) Prior to and during the DUB assay USP48 was subjected to in vitro phosphorylation by recombinant CK2. (D) Model for the impact of CSN-associated USP48 on RelA nuclear turnover. (1) USP48 stabilizes RelA upon its cytokine-induced nuclear entry, facilitating RelA nuclear accumulation. (2) USP48 Ub-chain-trimming activity is (transiently) enhanced upon its phosphorylation by CK2. (3) USP48 is inactivated by dephosphorylation and/or release from RelA and the CSN. (4) In absence of USP48, RelA becomes efficiently polyubiquitinated by ECS^{SOCS1} and subsequently degraded via the UPS in PML nuclear bodies.

resistant to labeling with HA-Ub-VS, and (II) a second Cys, susceptible for HA-Ub-VS labeling, but only when the catalytic site Cys is occupied with Ub-aldehyde, was described for Otu1 [42]. Although engagement of both Cys residues in catalysis was not reported, this feature of Otu1 somehow reminds of USP48: the latter being amenable for HA-Ub-VS-labeling (and possessing low peptidase activity independent of catalytic site Cys C98) in the absence of CK2-mediated phosphorylation but becoming labeling resistant (peptidase inactive) upon phosphorylation and the presence of long Ub-chains (>Ub_4). Both enhance USP48's isopeptidase/Ub-chain trimming activity, which essentially depends

on Cys C98. However, differential dependence of USP48 peptidase and isopeptidase/Ub-chain-trimming activity on alternate catalytic site Cys residues, an issue outside the focus of our study, requires further exploration through e.g. structural biology.

3.3. CSN and USP48 cooperatively control the nuclear turnover of RelA

In response to TNF stimulation, ubiquitination and UPS-dependent degradation of activated RelA proceed in the insoluble nuclear fraction enriched for PML and subunits of the 20S proteasome (Figs. 1A–C and S1A). This fraction likely corresponds to PML nuclear bodies [43], dynamic subnuclear compartments representing centers for proteolytic degradation upon response to various stresses [44,45]. Concordant with previous reports [4,5] we identified ECS^{SOCS1} as Ub-E3 for RelA and observed ECS^{SOCS1} subunits to accumulate in the nucleus upon cell treatment with TNF and LMB (Fig. 2D, E). CRL-dependent ubiquitination and TNF-induced association of RelA with the CSN in the nucleus (Figs. 1A and 3A, C) suggested the CSN, a master regulator of CRLs, to be decisively involved in the control of RelA nuclear turnover. Congruently, enhanced RelA-Ub accumulation was observed in CSN-depleted cells stimulated with TNF in the presence of MG132 (Fig. 2A), which indicated the CSN to act as an antagonist of RelA ubiquitination through either CRL inactivation (deneddylation) or RelA deubiquitination by an associated DUB.

Through a siRNA screen we identified USP48 as most promising DUB candidate regulating the nuclear turnover of RelA. USP48 and the CSN constitutively interact in the nucleus. Upon TNF-induced nuclear entry they immediately associate with RelA to collaboratively promote its nuclear accumulation and antagonize its polyubiquitination and degradation via the UPS. Our data are thus consistent with the CSN stabilizing RelA through an associated DUB. The association of USP48 with RelA is likely strengthened upon RelA ubiquitination. Through binding-mediated occlusion of short Ub-chains (up to Ub_4) attached to RelA, USP48 might prevent RelA-Ub capture by the UPS, thus stabilizing RelA independent of catalytic activity (Fig. 4B). Ub-chain elongation however is antagonized by USP48 Ub-chain trimming activity, which, likely through conformational rearrangement, is promoted upon USP48 Ub-chain-binding. CK2-mediated phosphorylation of USP48 at C-terminal CK2 consensus sites, in vitro and in response to TNF, enhances its Ub-chain-trimming activity (Fig. 8A–C). In response to TNF however, phosphorylation of USP48 is transient (Fig. 8C). Thus, dephosphorylation of USP48 and/or its release from RelA and the CSN through an unknown mechanism finally allow efficient polyubiquitination of RelA by ECS^{SOCS1}, mediating its proteasomal degradation (Fig. 8D). Interestingly, association of CK2 with the CSN and CK2-mediated phosphorylation of its subunits CSN2 and CSN7 have been observed [46], implying potential reciprocal regulation of CK2 and CSN activities, which might impact on timing of USP48 phosphorylation, Ub-chain trimming activity and association with the CSN. Although CK2, a highly conserved protein kinase with brought substrate specificity and pronounced pro-proliferative and anti-apoptotic activities, is widely viewed as constitutively active messenger-independent enzyme [47], a multitude of mechanisms potentially contributing to keep its activity in check in vivo, including regulated localization/turnover and association with other proteins, have been suggested [48].

In summary, we hypothesize one profession of USP48 to be protection of either the entire nuclear or the nucleoplasmic pool of RelA, as opposed to the chromatin-bound fraction being just yet transcriptionally engaged [49], from premature degradation via the UPS, thus extending the timespan of RelA's availability for transcriptional engagement. This might be of paramount importance, since induction of individual inflammatory genes is subject to divergent temporal control on multiple levels, but in each case essentially requires timely and dynamic supply of NF-κB (RelA) for transcription to proceed [50,51]. Short Ub-chains attached to RelA might either persist or be removed by other DUBs, e.g. USP7 [37], upon transcriptional engagement and "DUB exchange". The presence of short Ub-chains on RelA, shielded from or just below the threshold for capture by the proteasome, could enhance the promptness of RelA degradation at appropriate times.

4. Materials and methods

4.1. Eukaryotic expression constructs

A true ORF clone encoding full length *usp48* attributed with a C-terminal Myc-Flag-tag, integrated into the pCMV6Entry vector, was purchased from *Origene*. The expression construct for RelA was generated by cloning the PCR-amplified cDNA encoding for human *relA* into the pcDNA™3.1 expression vector (*Invitrogen*). In addition, a sequence encoding the His_6-tag and the T7-tag was included in the 5′-end PCR primers. Constructs for USP48-FL and the USP48 CD (aa 1–450), attributed with an N-terminal Flag-tag were generated by integrating the PCR-amplified ORF encoding for human FL *usp48* or a shorter fragment encoding for the *usp48* CD into the pENTR™-SD/D-TOPO® vector (*Invitrogen*). Additionally, a sequence encoding the Flag-tag was attached to the 5′-end PCR primers. Exploiting the Gateway® system (*Invitrogen*), the cDNA ORFs integrated in the pENTR™-SD vector were then subcloned into the pCDNA™3.2/V5-DEST expression vector (*Invitrogen*). $USP48^{C98A}$ with the catalytic site Cys mutated to Ala, and a USP48-FL CK2 phosphosite mutant ($USP48^{PS\text{-}Mut.}$) with serines 886–888 and Thr 890 all mutated to alanine, both possessing a C-terminal Myc-Flag-tag, were generated by site-directed mutagenesis (GeneArt® Site-Directed Mutagenesis Plus Kit, *Life Technologies*). All constructs generated during this study were verified by sequencing (*GATC Biotech*).

4.2. Recombinant proteins and human purified CSN

Recombinant proteins were obtained from following sources: CK2 (*New England Biolabs*), GST (*GeneScript*), Flag-Myc-RelA (*OriGene*), human COP9 signalosome (hCSN) purified from erythrocytes, His_6-UCHL3 and His_6-USP15 (*ENZO Life Sciences*), His_6-USP7-FL and USP5/isopeptidase T-FL (*Boston Biochem*) and GST-USP48-FL (*Abnova*). GST-USP48-CD (USP48 catalytic domain, aa 1–450) and $GST\text{-}USP48^{C98A}$ were custom-cloned and synthesized using a wheat germ-based in vitro translation system followed by affinity purification (*Abnova*). Constructs were verified by sequencing (*Abnova*).

4.3. Cell culture, cell treatments and transfection

HeLa (CCL2) cells (*ATCC*) and HEK293 cells (ATTC) were cultured in RPMI 1640 medium (*PAA*), supplemented with FCS (10%, *Biochrom*), HEPES (20 mM) and Penicillin/Streptomycin (100 U/ml, *PAA*). At least 24 h prior to transfection or stimulation with TNF (10 ng/ml, *R&D Systems*) or IL-1β (15 ng/ml, *Peprotech*) cells were seeded on Petri-dishes. 4 h–16 h prior to treatments they were transferred into medium free of serum and antibiotics (OptiMEM, *Life Technologies*). Transient transfections for protein overexpression were carried out in OptiMEM medium using 3–5 μg cDNA per 100 mm diameter dish and the Effectene transfection kit (*Qiagen*). 6 h post-transfection fresh medium with FCS was added and cell culture continued for 20 h. Transient knockdown of proteins of interest by siRNA was performed as described previously [8] using siRNA duplexes at a final concentration of 50–75 nM and the SiLentFect Lipid Reagent (*Bio-RAD*). A non-targeting siRNA (*Eurogentec or Life Technologies*, depending on the source of the targeting siRNA) was used as control. Cells were harvested the 3rd day after siRNA transfection or at times indicated in the figures. Most siRNA duplexes were custom designed and purchased from *Eurogentec*. A predesigned Silencer® Select siRNA targeting USP48 was bought from *Life Technologies*. siRNA sequences and order details are listed separately (Table S1). CHX (*Sigma*), MG132 (*Tocris*), LMB (*Calbiochem*) and ZVAD-

fmk (*BD Pharmingen*) were used at final concentrations of 25 μg/ml, 25 μM, 10 ng/ml and 10 μM respectively.

4.4. Cell proliferation assay

To analyze the impact of siRNA treatment on cell proliferation/viability, the Cell Titer-Glo® Luminescent Cell Viability Assay (*Promega*) was used according to the manufacturer's instructions. In brief: One day after targeting/non-targeting siRNA transfection, cells were harvested by trypsination and equal cell numbers (10,000/well) seeded in quadruplicate on white, flat, clear bottom 96 well plates in a volume of 100 μl. At least 4 h prior to analysis at day 1 to 4 (24–96 h) after cell seeding, the culture medium was replaced by 40 μl fresh medium/well. Assays were then performed according to instructions and read on a Spectramax M5 plate reader (*Molecular Devices*) equilibrated to 25 °C and set to detect luminescence at all wavelength with an integration time of 500 msec and a settling time of 100 msec in an endpoint measurement. Obtained results were blank-subtracted against cell-free culture medium. Applying the assay to a 1:2 serial dilution of HeLa cells, the assay was calibrated to determine cell numbers. A linear relationship between cell number and luminescence signal was obtained for up to 90,000 cells per well. In parallel, viability of siRNA-transfected cells, seeded on 60 mm diameter petri dishes and harvested by trypsination at days 1 to 4 after seeding, was determined using Countess Cell Counter (*Life Technologies*). At day 3 post transfection RIPA lysates (see below) were prepared from harvested cells to confirm knockdown success by immunoblot (IB).

4.5. Apoptosis assay

Induction of apoptosis by cell treatment with TNF and CHX was determined by use of the Caspase-Glo® 3/7 Assay (*Promega*) according to the manufacturer's instructions. In brief: One day after targeting/non-targeting siRNA transfection, cells were harvested by trypsination and 10,000 cells/well seeded in triplicate per experimental sample on a white, flat, clear bottom 96 well plate in a volume of 100 μl complete cell culture medium. At least 12 h prior to cell treatment with TNF and CHX after pre-incubation or not for 1 h with pan-caspase inhibitor ZVAD-fmk, as indicated in the figure, cell culture medium was replaced by 40 μl OptiMEM medium supplemented with 0,1% FCS per well. All reactions were stopped simultaneously through addition of an equal volume of Glo-Reagent pre-adapted to 25 °C and reactions subsequently incubated for 10 min with continuous shaking on a plate shaker at 25 °C. Luminescence generated was afterwards immediately read on a Spectramax M5 plate reader, using the settings described in the upper paragraph. Results were blank-subtracted against cell-free medium supplemented with vehicle (DMSO). Knockdown success was confirmed by IB analysis of RIPA lysates generated from cells, which had been seeded in parallel on 60 mm diameter petri dishes. Statistical significance of data obtained from 3 independent experiments was analyzed applying paired Student's *T*-test.

4.6. Preparation of whole cell extracts

Cells grown on Petri-dishes (10 cm diameter) were washed twice in ice-cold PBS and then scraped into 450 μl RIPA buffer (50 mM Tris (pH 7.5), 5 mM EDTA, 150 mM NaCl, 10 mM K_2HPO_4, 10% Glycerol, 1% Triton X-100 and 0.05% SDS), supplemented with 20 mM NaF, 1 mM Na_3VO_4, 1 mM Na_2MoO_4, 20 mM 2-phospho-glycerate (2-PG), 1 mM AEBSF and 1× EDTA-free protease inhibitor cocktail (PI/*Roche*). Lysates were incubated for 10 min on ice and cell lysis completed by passing them 5 times through a 27-gauge injection needle. Afterwards, lysates were cleared by centrifugation (13,000 ∗*g*, 4 °C, 10 min). The following compounds were added to the RIPA buffer when required, as indicated in the figure legends: N-ethyl-maleimide (NEM, 7.5 mM, *Fluka*), 1,10-*ortho*-phenanthroline (OPT, 5 mM, *Sigma*) and MG132 (25 μM). In experiments, where preservation of USP48 catalytic activity was required, RIPA buffer was replaced by Igepal lysis buffer (25 mM HEPES (pH 7.5), 150 mM NaCl, 5 mM EDTA, 10% Glycerol and 0.5% Igepal (*Sigma*)), only supplemented with 1 mM DTT, 1 mM AEBSF (*AppliChem*) and 25 μM MG132. LMB was only used in experiments with cytokine stimulation and cell harvest by subcellular fractionation (see below).

4.7. Subcellular fractionation

Cells grown on Petri-dishes (10 cm diameter) were washed twice with ice-cold buffer A (10 mM Tris (pH 7.9), 10 mM KCl, 1.5 mM $MgCl_2$, 10 mM K_2HPO_4, and 10% Glycerol) devoid of inhibitors and subsequently scraped into 450 μl pre-chilled buffer A supplemented with DTT (0.5 mM), AEBSF (1 mM), PI/*Roche* (1×), 2-PG (20 mM), NaF (20 mM), Na_3VO_4 (1 mM) and Na_2MoO_4 (1 mM). Cell suspensions were incubated for 10 min on ice to allow the cells to swell. Afterwards, 1 μl of 12.5% Igepal was added per 100 μl cell suspension to initiate cell lysis, which was allowed to proceed for 5 min on ice with incidental shaking. Nuclei were separated from cytosolic supernatants by centrifugation (2000 ∗*g*, 4 °C, 10 min) and cytosolic fractions afterwards cleared (13,000 ∗*g*, 4 °C, 10 min). Nuclear pellets (P1) were washed once in buffer A (300 μl) and then resuspended in 50 μl buffer C (20 mM Tris (pH 7.9), 420 mM NaCl, 1.5 mM $MgCl_2$, 0.2 mM EDTA, 10 mM K_2HPO_4, and 10% Glycerol), supplemented as described for buffer A, to extract soluble nuclear proteins (N1). After incubating the samples for 30 min on ice with incidental shaking, N1 fractions were harvested by centrifugation (13,000 ∗*g*, 4 °C, 10 min). Pellets (P2) were resuspended in 50 μl buffer E (20 mM Tris (pH 8.0), 150 mM NaCl, 1% (w/v) SDS, 1% (v/v) Igepal and 10 mM iodacetamide), supplemented as described for buffer A, with DTT omitted. Directly before use, buffer E was additionally supplemented with *Benzonase® Nuclease* (25 U/ml, *Novagen*). After incubating the samples for 30 min on ice with incidental shaking to extract insoluble nuclear proteins (N2) and to digest chromatin, N2 fractions (supernatants) were harvested by centrifugation (13,000 ∗*g*, 4 °C, 10 min) and pellets (P3) discarded. Total nuclear extracts (N_ts) containing both, soluble and insoluble nuclear proteins were prepared by directly extracting buffer A-washed nuclear pellets (P1) in buffer E with supplements. The following compounds were added where required to the fractionation buffers, as indicated in the figure legends: NEM (7.5 mM), OPT (5 mM), MG132 (25 μM) and LMB (10 ng/ml, only buffer A). In experiments where USP48 catalytic activity needed to be preserved, HEPES- instead of Tris-based buffers without any supplements, except DTT (0.5 mM), AEBSF (1 mM) and MG132 (25 μM) were used. Protein concentrations were determined by use of *Bio-RAD* Protein Assay (*Bio-RAD*) according to the manufacturer's instructions.

4.8. Immunoprecipitation and Western Blot

For IPs from whole cell extracts (WCEs) or cytosolic fractions equal amounts of protein (0.5–1 mg in a volume of 400 μl) were diluted (1:2) with IP buffer (20 mM Tris or HEPES (pH 7.4), 150 mM NaCl, 2 mM EDTA and 0.05% Triton X100) supplemented with AEBSF (1 mM), PI/*Roche* (1×), 2-PG (20 mM), NAF (20 mM), Na_3VO_4 (1 mM) and Na_2MoO_4 (1 mM). 1 μg protein-specific antibody (or 2.5 μl CSN1 antibody, *ENZO Life Sciences*) was added per reaction and samples incubated 4 h to over-night on a permanent rotator (7 rpm) at 4 °C. Afterwards, reactions were loaded on protein G sepharose beads (*GE Healthcare*, 25 μg per reaction), which had been previously four times washed in 800 μl IP buffer supplemented with PI/*Roche* (1×). Immune complex immobilization was allowed to proceed for 2 h at 4 °C. After centrifugation (500 ∗*g*, 2 min, 4 °C), supernatants were discarded and immune complexes 4–6 times washed in 800 μl IP buffer containing all inhibitors (500 ∗*g*, 2 min, 4 °C). After complete removal of the supernatants, beads were suspended in 40 μl 2× *Laemmli* sample buffer and β-ME (2.5 μl) added. Afterwards, samples were incubated with continuous shaking

(30 min, 56 °C), boiled (5 min, 95 °C) and centrifuged. Eluted immune complexes were recovered and analyzed by SDS PAGE and IB. For analysis of protein ubiquitination, the IP buffer was additionally supplemented with NEM (7.5 mM), OPT (5 mM) and MG132 (25 μM). In case of USP48-IP from WCEs, intended for subsequent use in DUB assays, the IP buffer, including supplements, was replaced by Igepal lysis buffer (refer to "preparation of whole cell extracts"). In case of T7(RelA)-IPs, protein G sepharose beads were pre-loaded with T7-antibody (1 μl per reaction). For Flag(USP48)-IPs Flag-agarose beads (*Sigma*) were used. In both cases, diluted samples were directly applied to washed antibody-loaded beads (25 μg per reaction), rotated 4 h to over-night and captured immune complexes handled as described above. Nuclear fractions were diluted with salt- (N1) or detergent-free buffer (N2, N_t) prior to IP to regenerate salt (N1) or detergent concentrations (N2, N_t) compatible with immune complex formation. Equal amounts of protein (200–500 μg) were then used per IP reaction and IPs performed as described. To suppress unspecific protein binding to beads, captured immune complexes were washed twice in IP buffer with increased salt (up to 300 mM NaCl) or Igepal concentration (up to 0.5% v/v), where required, before the standard washing procedure was performed. Prior to application of IPs to trap-tag-labeling reactions or DUB assays, they were additionally washed twice in DUB assay buffer, supplemented with protease inhibitors (refer to later paragraphs).

Samples (10 μg protein per lane, or equal aliquots of DUB assays or IPs) were separated on SDS-PAGE gels and transferred to PVDF membranes (*Millipore*). SeeBlue® Plus2 pre-stained standard (*Life Technologies*) was additionally run as MW marker on each gel. IB detections were performed using antibodies, as indicated in the figures and listed separately (Tables S2 and S3), and either Amersham ECL™ Western Blotting Detection Reagents (*GE Healthcare*) or the SuperSignal® West Dura Extended Duration Substrate Kit (*Thermo Scientific*). Images of IBs were obtained by film development, followed by film scanning, or captured by use of a CCD camera-based gel/blot imaging system (*Chemostar Professional, INTAS*). Densitometric analysis of scans or raw images was performed with *Image Studio Lite 3.1 (Licor)*. For visual presentation images were processed with *Photoshop 11.0.2.*

4.9. Pulldown assays with recombinant proteins or purified CSN

Equal molar amounts [μg] of recombinant proteins or purified hCSN, as indicated in the figures (Figs. 3D–F and S3C, D) were coincubated in HEPES-based IP buffer supplemented with PI/*Roche* (1×), AEBSF (1 mM), 2-PG (20 mM) and Prionex (0.1%, *Polysciences*) for 2 h at 4 °C with continuous shaking in a final reaction volume of 100 μl. Afterwards, reactions were loaded on either anti-Flag(M2) agarose or protein G sepharose beads (40 μl 50% beads per reaction) preloaded with anti-GST antibody (1 μg per reaction), as indicated in the figures. Prior to their use for IP, free protein binding sites of antibody-loaded beads were blocked by rotating the beads in IP buffer additionally supplemented with 1.5% Prionex (2 h, 4 °C, 7 rpm). Afterwards, beads were washed and then resuspended in 100 μl IP-Puffer containing 0.49% Prionex. Protein reactions were then added to the beads, resulting in a final reaction volume of 200 μl and a final Prionex concentration of 0.25%. IP reactions were rotated for 2 h at 4 °C and 7 rpm. After four washes in IP buffer (2 min, 4 °C, 500 $*g$), supernatants were completely removed and discarded. Captured immune complexes were eluted by shaking the beads in 30 μl 2× *Laemmli* buffer supplemented with 2.5 μl β-ME per reaction (5 min, 95 °C). Eluted immune complexes were harvested by centrifugation and equal aliquots of samples analyzed by SDS-PAGE and IB, as indicated in the figures.

4.10. Trap-tag-labeling of DUBs

Trap-tag-labeling of recombinant DUBs or DUBs immunoprecipitated from cells was adapted from literature [52]. Recombinant DUBs (0.5 μM) were preincubated for 5 min at 30 °C with continuous shaking in DUB assay buffer (50 mM HEPES (pH 7.5) with 100 mM NaCl), supplemented with DTT (1 mM) and AEBSF (1 mM) in the presence or absence of Ub-VS (15 μM), Ub-VME (15 μM), both obtained from *Boston Biochem*, NEM (10 mM), ATP (200 μM), $MgCl_2$ (2 mM) and/or CK2 (0.5 U/15 μl reaction, *New England Biolabs*), as indicated in the figures. After 5 min, HA-Ub, HA-Ub-VS or HA-Ub-VME (3 μM, *ENZO Life Sciences*) were added, as indicated in the figures, and labeling reactions allowed to proceed for 1 h at 30 °C with continuous shaking in a reaction volume of 15 μl. Afterwards, 5 μl 4× *Laemmli* sample buffer and 1.5 μl β-ME were added per reaction and samples boiled (5 min, 95 °C). Equal aliquots of all reactions were analyzed by SDS-PAGE and IB, by the use of the indicated antibodies. For labeling of DUBs (endogenous or ectopically expressed) immunoprecipitated from cell extracts, MG132 (25 μM) was additionally added to the labeling reactions.

4.11. In vitro DUB assay

For kinetic Ub_4 DUB assays, recombinant DUBs (0.5 μM) were preincubated for 5 min at 30 °C with continuous shaking in DUB assay buffer supplemented with DTT (1 mM) and AEBSF (1 mM). Ub_4 of different linkage types was then added (3 μg) and incubation of all reactions (30 μl) continued for up to 60 min at 30 °C with continuous shaking. At various times aliquots (6.5 μl) were taken from each reaction, combined with 8.5 μl 2× *Laemmli* sample buffer and 1.5 μl β-ME, boiled (5 min, 95 °C), centrifuged and stored at −80 °C. Equal aliquots of all samples were separated by SDS-PAGE and analyzed by IB.

Endpoint DUB assays using either recombinant USP48 variants (0.5 μM) or USP48 variants immunoprecipitated from cell extracts as DUB source and either ubiquitinated immunoprecipitated RelA or Ub-chains of different linkage types as DUB substrate (Ub_4 (1.5 μg) or Ub_{3-7} (1.9 μg)), were performed in the presence or absence of NEM (10 mM) in a final reaction volume of 15 μl. In case of Ub_{3-7}-chains an average MW of 40 kDa was assumed to calculate molarities. Reactions were stopped after 1.5–2 h incubation by addition of 5 μl 4× *Laemmli* sample buffer and 2 μl β-ME and then boiled (5 min, 95 °C). Afterwards, samples were handled as described above. In some cases SDS-PAGE-separated samples were additionally analyzed by SYPRO Rubi gel stain (*Bio-RAD*), which was performed according to the manufacturer's instructions. Images of SYPRO-Rubi-stained gels were captured using the *Chemostar Professional* imaging system equipped with a 312 nm UV transilluminator for excitation and a SYPRO-Rubi emission filter (*INTAS*).

4.12. Luminescence assay for DUB activity

Luminescence assays for DUB activity were performed using the DUB-Glo™ Protease Assay Kit (*Promega*) as described [53]. The luminogenic substrate (Z-RLRGG-aminoluciferin) provided with the kit was replaced by Ub-AML (*Boston Biochem*). Serial (1:2) dilutions of DUBs prepared in DUB assay buffer, supplemented with DTT (2 mM), AEBSF (1 mM) and Prionex (0.1%), were placed into wells of white opaque 96 well half area plates (*Greiner*, 30 μl reaction volume). Plates were then prewarmed (5 min, 30 °C) with continuous shaking. Afterwards, 30 μl DUB-Glo™ reagent supplemented with Ub-AML (0.5 μM) was added to each reaction, generating the final concentration of Ub-AML (250 nM) and the final concentrations of the DUBs, as indicated in the figures (Figs. 5A and S5-1A–G). Reactions were immediately monitored for 45 min on a Spectramax M5 plate reader with readings taken every 20 s to 1 min and the reader set to detect luminescence at all wavelengths with an integration time of 500 msec. On each plate reactions were performed in duplicate. After data export to *Excel*, plots of kinetic measurements were generated with each data point representing the mean of two replicates. Relative luminescence (RLU) values peaked after about 3 min, depending on DUB type and DUB concentration. From each serial DUB dilution the RLU value at peak level was determined. For each DUB analyzed, these values were then plotted against DUB concentration and graphs fitted by linear regression.

4.13. FRET-TAMRA/QXL570-di-Ub fluorescence assay for DUB activity

DUB assays with FRET-based Ub_2-substrates were adapted from literature [54]. Dilutions of recombinant DUBs (15 μl) in DUB assay buffer, supplemented with DTT (1 mM) and AEBSF (1 mM), were placed in duplicate into wells of a black opaque 96 well half area plate (*Greiner*) and the plate then prewarmed (5 min, 30 °C) with continuous shaking. Afterwards, an equal volume of FRET-TAMRA/QXL570 Ub_2-substrates (*Boston Biochem*) of different linkage type (K48, K63 or K11) and labeling position for the fluorescent dye TAMRA and the quencher molecule QXL570 (P1-P4, Figs. 5B and S5-2A–F), prepared in DUB assay buffer (200 nM) as well, was added to each well, resulting in the final concentration of the Ub_2-substrates (100 nM) and the final concentrations of the DUBs, as indicated in the figures, in a reaction final volume of 30 μl. Kinetics of substrate conversion in each well was then immediately monitored on a Spectramax M5 plate reader set to detect fluorescence at ex544 nm and em572 nm for 60 min. A reading was taken every 20 s without time delay. Data were exported to *Excel* and plots for time-dependent substrate conversion in each reaction generated. A calibration curve for the fluorescence increase resulting from TAMRA-Ub release upon Ub_2-cleavage by DUBs was established by the use of 5-TAMRA-Lys(Ub)-Gly-OH (*Boston Biochem*) and exploited to convert measured relative fluorescence units (RFU values) into the amount of TAMRA-Ub generated [nM]. Finally, initial catalytic rates [s^{-1}] at the fixed substrate concentration (100 nM) were calculated for each DUB analyzed by division of the determined initial cleavage velocity by enzyme concentration.

4.14. Polymerase chain reaction

RNA was extracted from $5 * 10^6$–$1 * 10^7$ cultured cells using the InnuPREP RNA Mini Kit (*Analytik Jena*). Per reaction 1.5 μg RNA were reverse transcribed using MMLV reverse transcriptase and the First Strand cDNA Synthesis Kit (*Thermo Scientific*). RT-qPCRs were run on a StepOnePlus™ real time qPCR platform (*Applied Biosystems*) by the use of 1 μl cDNA per reaction, target gene-specific primer pairs and the SensiMix™ SYBR Kit (*Bioline*). Per 96 well PCR plate samples were analyzed in duplicate for at least one target gene of interest and *gapdh*, used as reference gene for normalization. In addition, relative cDNA calibration curves for both, target gene(s) of interest and *gapdh* were run on each plate. Relative quantities of the target gene(s) of interest and *gapdh* were then determined by use of their respective calibration curves and the results obtained for the gene(s) of interest normalized against those obtained for *gapdh*. Afterwards, relative changes in target gene expression, e.g. during a time course of TNF-stimulation, were determined by dividing the result obtained for each sample by the result obtained for the reference sample (usually the sample generated from non-transfected and non-stimulated cells). RT-qPCR specificity was controlled by no-template and no-RT samples, as well as by melting curve analysis. Sequences of human gene-specific primer pairs used in the study are provided separately (Table S4).

4.15. CK2 kinase assay

Recombinant CK2 (0.5 U/reaction) was preincubated for 10 min at 30 °C with continuous shaking in DUB assay buffer supplemented with DTT (5 mM), AEBSF (1 mM), ATP (200 μM) and $MgCl_2$ (2 mM) in the presence or absence of CK2 inhibitor VIII (1 μM). Afterwards, recombinant GST or GST-tagged USP48 variants (GST-USP48-FL or GST-USP48-CD) were added and kinase reactions (15 μl final) performed for 1 h at 30 °C with continuous shaking. After 1 h, reactions were put on ice, supplemented with 5 μl 4× *Laemmli* sample buffer and 2 μl β-ME and then boiled (5 min, 95 °C). Equal aliquots of all samples were separated by SDS-PAGE and analyzed by IB. Kinase reactions with endogenous USP48 or epitope-tagged USP48 variants as the substrate, after their overexpression in HeLa cells and anti-Flag-IP from N1 nuclear fractions, were performed as follows: recombinant CK2, pre-incubated for 10 min in a reaction volume of 15 μl in the presence of DTT (5 mM), AEBSF (1 mM), MG132 (25 μM), ATP (200 μM), $MgCl_2$ (10 mM) and CK2 inhibitor VIII (1 μM), as indicated in the figures (Figs. 6B and 8A, B), was added to washed IPs and samples then incubated for 1 h at 30 °C and further handled as described above.

4.16. RNAi DUB screen

To identify candidate DUBs potentially involved in the regulation of nuclear NF-κB, a Silencer® select/Silencer siRNA DUB screen was established/valuated in cooperation with and then performed by *Cenix BioScience GmBH* (Dresden, Germany). In brief, each of the 100 target genes, encompassing all assigned human DUBs, as well as positive and negative controls, was screened by 3 individual siRNAs (*Life Technologies*) in experimental triplicates. As a readout, nuclear translocation of RelA 30 and 60 min post TNF (10 ng/ml) stimulation was determined by fluorescence microscopy (Hoechst stain/NF-κB assay). Visual image quality control (QC) was performed with Metamorph (MDC) software and automated quantitative image analysis by the use of the eCognition (Definiens) software. In addition, in RT-qPCR assays, induction of the NF-κB target genes IL-8 and IL-6 after 30 and 60 min of TNF stimulation was analyzed. QC of the screening data indicated that the screening was performed successfully under technically sound conditions. The ranking of candidate hit genes was done using the "redundant siRNA activity" (RSA) methodology [55].

Abbreviations list

AML	aminoluciferin
Atx3	ataxin-3
CK2	casein-kinase-2
CD	catalytic domain
CSN	COP9 signalosome
COMMD1	copper metabolism Murr1 domain-containing protein 1
Cul	cullin
CRL	Cul-RING-Ub-ligase
CHX	cycloheximide
EloB	elongin B
DUB	deubiquitinase
FL	full length
HMW	high molecular weight
IP	immunoprecipitation
IB	immunoblot
IκB	inhibitor of NF-κB
JAMM/MPN$^+$ motif	JAB1/MPN/MOV34 motif
LMB	leptomycin B
NEM	N-ethylmaleimide
NF-κB	nuclear factor kappa B
OPT	*ortho*-phenanthroline
OTU1	otubain-1
Ub	ubiquitin
UCH	Ub c-terminal hydrolase
Ub-E3	Ub ligase
UPS	Ub proteasome system
USP	Ub-specific peptidase
VS	vinylsulfone
VME	vinylmethylester

Acknowledgments

The work was supported in part by a DFG grant to M.N. (Na 292/7). We thank C. Wolf, M. Borgmann and A. Ghanem for the assistance in PCR analysis, cloning and site-directed mutagenesis.

Appendix A. Supplementary data

Supplemental information encompassing seven figures (Figs. S1 to S5-3) and four tables(Tables S1 to S4) is available at *BBA Mol. Cell Res.* online at http://dx.doi.org/10.1016/j.bbamcr.2014.11.028.

References

[1] N.D. Perkins, The diverse and complex roles of NF-κB subunits in cancer, Nat. Rev. Cancer 12 (2012) 121–132.
[2] M.S. Hayden, S. Ghosh, Shared principles in NF-κB signaling, Cell 132 (2008) 344–362.
[3] S. Saccani, I. Marazzi, A.A. Beg, G. Natoli, Degradation of promoter-bound p65/RelA is essential for the prompt termination of the nuclear factor κB response, J. Exp. Med. 200 (2004) 107–113.
[4] A. Ryo, F. Suizu, Y. Yoshida, K. Perrem, Y.-C. Liou, G. Wulf, R. Rottapel, S. Yamaoka, K.P. Lu, Regulation of NF-κB signaling by Pin1-dependent prolyl isomerization and ubiquitin-mediated proteolysis of p65/RelA, Mol. Cell 12 (2003) 1413–1426.
[5] G.N. Maine, X. Mao, C.M. Komarck, E. Burstein, COMMD1 promotes the ubiquitination of NF-κB subunits through a cullin-containing ubiquitin ligase, EMBO J. 26 (2007) 436–447.
[6] C. Schwechheimer, The COP9 signalosome (CSN): an evolutionary conserved proteolysis regulator in eukaryotic development, Biochim. Biophys. Acta 1695 (2004) 45–54.
[7] K. Schweitzer, M. Naumann, Control of NF-κB activation by the COP9 signalosome, Biochem. Soc. Trans. 38 (2010) 156–161.
[8] K. Schweitzer, P.M. Bozko, W. Dubiel, M. Naumann, CSN controls NF-κB by deubiquitinylation of IκBα, EMBO J. 26 (2007) 1532–1541.
[9] V. Welteke, A. Eitelhuber, M. Düwel, K. Schweitzer, M. Naumann, D. Krappmann, COP9 signalosome controls the Carma1-Bcl10-Malt1 complex upon T-cell stimulation, EMBO Rep. 10 (2009) 642–648.
[10] C. Zhou, S. Wee, E. Rhee, M. Naumann, W. Dubiel, D.A. Wolf, Fission yeast COP9/signalosome suppresses cullin activity through recruitment of the deubiquitylating enzyme Ubp12p, Mol. Cell 11 (2003) 927–938.
[11] B.K.J. Hetfeld, A. Helfrich, B. Kapelari, H. Scheel, K. Hofmann, A. Guterman, M. Glickman, R. Schade, P.M. Kloetzel, W. Dubiel, The zinc finger of the CSN-associated deubiquitinating enzyme USP15 is essential to rescue the E3 ligase Rbx1, Curr. Biol. 15 (2005) 1217–1221.
[12] J.-T. Wu, Y.-R. Chan, C.-T. Chien, Protection of cullin-RING E3 ligases by CSN-UBP12, Trends Cell Biol. 16 (2006) 362–369.
[13] R.J. Deshaies, E.D. Emberley, A. Saha, Control of cullin-RING ubiquitin ligase activity by NEDD8, Subcell. Biochem. 54 (2010) 41–56.
[14] S. Wee, R.K. Geyer, T. Toda, D.A. Wolf, CSN facilitates cullin-RING ubiquitin ligase function by counteracting autocatalytic adapter instability, Nat. Cell Biol. 7 (2005) 387–391.
[15] M.W. Schmidt, P.R. McQuary, S. Wee, K. Hofmann, D.A. Wolf, F-box-directed CRL complex assembly and regulation by the CSN and CAND1, Mol. Cell 35 (2009) 586–597.
[16] E.D. Emberley, R. Mosadeghi, R.J. Deshaies, Deconjugation of Nedd8 from Cul1 is directly regulated by Skp1-F-box and substrate, and the COP9 signalosome inhibits deneddylated SCF by a noncatalytic mechanism, J. Biol. Chem. 287 (2012) 29679–29689.
[17] D.A. Wolf, C. Zhou, S. Wee, The COP9 signalosome: an assembly and maintenance platform for cullin ubiquitin ligases? Nat. Cell Biol. 5 (2003) 1029–1033.
[18] G.A. Cope, R.J. Deshaies, COP9 signalosome: a multifunctional regulator of SCF and other cullin-based ubiquitin ligases, Cell 114 (2003) 663–671.
[19] F.E. Reyes-Turcu, K.H. Ventii, K.D. Wilkinson, Regulation and cellular roles of ubiquitin-specific deubiquitinating enzymes, Annu. Rev. Biochem. 78 (2009) 363–397.
[20] E.W. Harhaj, V.M. Dixit, Regulation of NF-κB by deubiquitinases, Immunol. Rev. 246 (2012) 107–124.
[21] L. Orel, H. Neumeier, K. Hochrainer, B.R. Binder, J.A. Schmid, Crosstalk between the NF-κB activating IKK-complex and the CSN signalosome, J. Cell. Mol. Med. 14 (2010) 1555–1568.
[22] J.-H. Lee, L. Yi, J. Li, K. Schweitzer, M. Borgmann, M. Naumann, H. Wu, Crystal structure and versatile functional roles of the COP9 signalosome subunit 1, Proc. Natl. Acad. Sci. U. S. A. 110 (2013) 11845–11850.
[23] A. Hoffmann, A. Levchenko, M.L. Scott, D. Baltimore, The IκB-NF-κB signaling module: temporal control and selective gene activation, Science 298 (2002) 1241–1245.
[24] D.E. Nelson, A.E.C. Ihekwaba, M. Elliott, J.R. Johnson, C.A. Gibney, B.E. Foreman, G. Nelson, V. See, C.A. Horton, D.G. Spiller, S.W. Edwards, H.P. McDowell, J.F. Unitt, E. Sullivan, R. Grimley, N. Benson, D. Broomhead, D.B. Kell, M.R.H. White, Oscillations in NF-κB signaling control the dynamics of gene expression, Science 306 (2004) 704–708.
[25] L. Ashell, C.A. Horton, D.E. Nelson, P. Paszek, C.V. Harper, K. Sillitoe, S. Ryan, D.G. Spiller, J.F. Unitt, D.S. Broomhead, D.B. Kell, D.A. Rand, V. See, M.R.H. White, Pulsatile stimulation determines timing and specificity of NF-κB-dependent transcription, Science 324 (2009) 242–246.
[26] M. Naumann, D. Bech-Otschir, X. Huang, K. Ferrell, W. Dubiel, COP9 signalosome-directed c-Jun activation/stabilization is independent of JNK, J. Biol. Chem. 274 (1999) 35297–35300.
[27] A. Peth, C. Berndt, W. Henke, W. Dubiel, Downregulation of COP9 signalosome subunits differentially affects the CSN complex and target protein stability, BMC Biochem. 8 (2007) 27.
[28] U. Leppert, W. Henke, X. Huang, J.M. Müller, W. Dubiel, Post-transcriptional fine-tuning of COP9 signalosome subunit biosynthesis is regulated by the c-Myc/Lin28B/let-7 pathway, J. Mol. Biol. 409 (2011) 710–721.
[29] C. Tzimas, G. Michailidou, M. Arsenakis, E. Kieff, G. Mosialos, E.G. Hatzivassiliou, Human ubiquitin-specific protease 31 is a deubiquitinating enzyme implicated in activation of nuclear factor-κB, Cell. Signal. 18 (2006) 83–92.
[30] D. Komander, M.J. Clague, S. Urbe, Breaking the chains: structure and function of the deubiquitinases, Nat. Rev. Mol. Cell Biol. 10 (2009) 550–563.
[31] D. Wissing, H. Mouritzen, M. Jäättelä, TNF-induced mitochondrial changes and activation of apoptotic proteases are inhibited by A20, Free Radic. Biol. Med. 25 (1998) 57–65.
[32] S. Daniel, M.B. Arvelo, V.I. Patel, C.R. Longo, G. Shrikhande, T. Shukri, J. Mahiou, D.W. Sun, J. Mottley, S.T. Grey, C. Ferran, A20 protects endothelial cells from TNF-, Fas-, and NK-mediated cell death by inhibiting caspase 8 activation, Blood 104 (2004) 2376–2384.
[33] M.W. Popp, K. Artavanis-Tsakonas, H.L. Ploegh, Substrate filtering by the active site crossover loop in UCHL3 revealed by sortagging and gain-of-function mutations, J. Biol. Chem. 284 (2009) 3593–3602.
[34] B.G. Burnett, R.N. Pittman, The polyglutamine neurodegenerative protein ataxin 3 regulates aggresome formation, Proc. Natl. Acad. Sci. U. S. A. 102 (2005) 4330–4335.
[35] J.S. Thrower, L. Hoffman, M. Rechsteiner, C.M. Pickart, Recognition of the polyubiquitin proteolytic signal, EMBO J. 19 (2000) 94–102.
[36] D. Komander, F. Reyes-Turcu, J.D.F. Licchesi, P. Odenwaelder, K.D. Wilkinson, D. Barford, Molecular discrimination of structurally equivalent Lys 63-linked and linear polyubiquitin chains, EMBO Rep. 10 (2009) 466–473 (alte Nr. 28).
[37] A. Colleran, P.E. Collins, C. O'Carroll, A. Ahmed, X. Mao, B. McManus, P.A. Kiely, E. Burstein, R.J. Carmody, Deubiquitination of NF-κB by ubiquitin-specific protease-7 promotes transcription, Proc. Natl. Acad. Sci. U. S. A. 110 (2013) 618–623.
[38] J.B. Schaefer, D.O. Morgan, Protein-linked ubiquitin chain structure restricts activity of deubiquitinating enzymes, J. Biol. Chem. 286 (2011) 45186–45196.
[39] S. Rumpf, S. Jentsch, Functional division of substrate processing cofactors of the ubiquitin-selective Cdc48 chaperone, Mol. Cell 21 (2006) 261–269.
[40] T.E. Messick, N.S. Russell, A.J. Iwata, K.L. Sarachan, R. Shiekhattar, J.R. Shanks, F.E. Reyes-Turcu, K.D. Wikinson, R. Marmorstein, Structural basis for ubiquitin recognition by the Otu1 ovarian tumor domain protein, J. Biol. Chem. 283 (2008) 11038–11049.
[41] C.A. Matos, S. de Macedo-Ribeiro, A.L. Carvalho, Polyglutamine diseases: the special case of ataxin-3 and Machado–Joseph disease, Prog. Neurobiol. 95 (2011) 26–48.
[42] T. Wang, L. Yin, E.M. Cooper, M.Y. Lai, S. Dickey, C.M. Pickart, D. Fushman, K.D. Wilkinson, R.E. Cohen, C. Wolberger, Evidence for bidentate substrate binding as the basis for the K48 linkage specificity of otubain 1, J. Mol. Biol. 386 (2009) 1011–1023.
[43] T. Tanaka, M.J. Grusby, T. Kaisho, PDLIM2-mediated termination of transcription factor NF-κB activation by intranuclear sequestration and degradation of the p65 subunit, Nat. Immunol. 8 (2007) 584–591.
[44] A. Mikecz, The nuclear ubiquitin-proteasome system, J. Cell Sci. 119 (2006) 1977–1984.
[45] R. Bernardi, P.P. Pandolfi, Structure, dynamics and function of promyeloic leukaemia nuclear bodies, Nat. Rev. Mol. Cell Biol. 8 (2007) 1006–1016.
[46] S. Uhle, O. Medalia, R. Waldron, R. Dumdey, P. Henklein, D. Bech-Otschir, X. Huang, M. Berse, J. Sperling, R. Schade, W. Dubiel, Protein kinase CK2 and protein kinase D are associated with the COP9 signalosome, EMBO J. 22 (2003) 1302–1312.
[47] J.S. Duncan, D.W. Litchfield, Too much of a good thing: the role of protein kinase CK2 in tumorigenesis and prospects for therapeutic inhibition of CK2, Biochim. Biophys. Acta 1784 (2008) 33–47.
[48] D.W. Litchfield, Protein kinase CK2: structure, regulation and role in cellular decisions of life and death, Biochem. J. 369 (2003) 1–15.
[49] D. Bosisio, I. Marazzi, A. Agresti, N. Shimizu, M.E. Bianchi, G. Natoli, A hyper-dynamic equilibrium between promoter-bound and nucleoplasmic dimers controls NF-κB-dependent gene activity, EMBO J. 25 (2006) 798–810.
[50] G. Natoli, Control of NF-κB-dependent transcriptional responses by chromatin organization, Cold Spring Harb. Perspect. Biol. 1 (2009) a000224.
[51] S.T. Smale, Selective transcription in response to an inflammatory stimulus, Cell 140 (2010) 833–844.
[52] A. Borodovsky, H. Ovaa, N. Kolli, T. Gan-Erdene, K.D. Wilkinson, H.L. Ploegh, B.M. Kessler, Chemistry-based functional proteomics reveals novel members of the deubiquitinating enzyme family, Chem. Biol. 9 (2002) 1149–1159.
[53] N. Russell, J.T. Brazell, C. Schwerdtfeger, H. Ovaa, F. Melandri, Fluorescence Polarization (FP) and Chemiluminescent Based Substrate Alternatives for Analyzing DUB Activity, 2011. (Poster distributed by Boston Biochem).
[54] C. Schwerdtfeger, F.E. Oualid, H. Ovaa, S. Gygi, F. Melandri, New discovery Platform Tools for Deubiquitinating Enzymes (DUBs), 2011. (Poster distributed by Boston Biochem).
[55] R. König, C.-Y. Chiang, B.P. Tu, S.F. Yan, P.D. DeJesus, A. Romero, T. Bergauer, A. Orth, U. Krueger, Y. Zhou, S.K. Chanda, A probability-based approach for the analysis of large-scale RNAi screens, Nat. Methods 4 (2007) 847–849.
[56] Y. Ye, H. Scheel, K. Hofmann, D. Komander, Dissection of USP catalytic domains reveals five common insertion points, Mol. BioSyst. 5 (2009) 1797–1808.
[57] Y. Xue, J. Ren, X. Gao, C. Jin, L. Wen, X. Yao, GPS 2.0, a tool to predict kinase-specific phosphorylation sites in hierarchy, Mol. Cell. Proteomics 7 (2008) 1598–1608.